CHARACTERIZATION OF SPRAY COOLING FOR ELECTRONIC DEVICES

A THESIS SUBMITTED TO
THE GRADUATE SCHOOL OF NATURAL AND APPLIED SCIENCES
OF
MIDDLE EAST TECHNICAL UNIVERSITY

BY

SELÇUK ÖKSÜZ

IN PARTIAL FULFILLMENT OF THE REQUIREMENTS
FOR
THE DEGREE OF MASTER OF SCIENCE
IN
MECHANICAL ENGINEERING

JANUARY 2014

Approval of the thesis:

CHARACTERIZATION OF SPRAY COOLING FOR ELECTRONIC DEVICES

submitted by **SELÇUK ÖKSÜZ** in partial fulfillment of the requirements for the degree of **Master of Science in Mechanical Engineering Department, Middle East Technical University** by,

Prof. Dr. Canan Özgen
Dean, Graduate School of **Natural and Applied Sciences** _____

Prof. Dr. Süha Oral
Head of Department, **Mechanical Engineering** _____

Dr. Tahsin Çetinkaya
Supervisor, **Mechanical Engineering Dept., METU** _____

Examining Committee Members:

Assoc. Prof. Dr. İlker Tarı
Mechanical Engineering Department, METU _____

Dr. Tahsin Çetinkaya
Mechanical Engineering Department, METU _____

Assist. Prof. Dr. Metin Yavuz
Mechanical Engineering Department, METU _____

Dr. Özgür Bayer
Mechanical Engineering Department, METU _____

M.Sc. Uğur Alakoç
Senior Expert Thermal Engineer, ASELSAN _____

Date: **21.01.2014**

I hereby declare that all information in this document has been obtained and presented in accordance with academic rules and ethical conduct. I also declare that, as required by these rules and conduct, I have fully cited and referenced all material and results that are not original to this work.

Name, Last Name: SELÇUK ÖKSÜZ

Signature   :

ABSTRACT

CHARACTERIZATION OF SPRAY COOLING FOR ELECTRONIC DEVICES

ÖKSÜZ, Selçuk

M.S., Department of Mechanical Engineering

Supervisor   : Dr. Tahsin Çetinkaya

January 2014, 73 pages

The trends in electronics industry are towards miniaturizing and increasing power needs that result in high heat fluxes. High heat fluxes lead to thermal problems and performance loss in devices. Well known cooling techniques, such as utilization of fans or single phase liquid cooling, have limited cooling capacity. Among two phase cooling methods, spray cooling is one of the best cooling technique. Thus, in this study it is aimed to construct a compact and high performance yet simple experimental setup for a real life application of spray cooling of high heat flux electronic devices.The closed loop system consists of a spraying chamber, a custom made microchannel heat exchanger as a condenser unit, a gear pump and a small filter-reservoir assembly. Dielectric liquid FC-72 is sprayed vertically upward using single pressure atomized nozzle to 20 mm diameter chamber. In these tests, two 10 Ω thick film resistors on a copper block are used to simulate high heat flux boundary condition. Ten different surface arrangements are tested by changing heat flux and volumetric flow rate of the spraying liquid. Experimental results show that at 0.4 liters/min flow rate, 130 W/cm^2 maximum heat flux (40.85% enhancement) is achieved with the

straight fin surface arrangement.

ÖZ

ELEKTRONİK CİHAZLAR İÇİN SPREY SOĞUTMA KARAKTERİZASYONU

ÖKSÜZ, Selçuk

Yüksek Lisans, Makina Mühendisliği Bölümü

Tez Yöneticisi   : Dr. Tahsin Çetinkaya

Ocak 2014 , 73 sayfa

Giderek küçülen yapılar ve artan güç ihtiyacı nedeniyle ortaya çıkan yüksek ısı akısı elektronik ürünlerde ısıl açıdan problemlere ve performans kayıplarına neden olmaktadır. Bugüne kadar birçok yerde kabul görmüş fanlı ya da tek fazlı sıvı soğutma sistemlerinin soğutma kapasitesi bu gibi durumlar için yetersiz kalmaktadır. Sprey soğutma teknolojisi, iki fazlı soğutma olmasıyla en iyi soğutma yöntemi olarak öngörülmektedir. Dolayısıyla bu çalışmada yüksek ısı akılı elektroniklerin bulunduğu günümüz sistemlerinde rahatlıkla kullanılabilecek küçük, basit ve yüksek performanslı bir deney düzeneği geliştirilmesi amaçlanmıştır. Bu kapsamda sprey odası, yoğuşturucu olarak kullanılan özel olarak üretilmiş mikrokanal ısı değiştiricisi, dişli pompa ve küçük boyutlarda bir filtre-rezervuar komplesinden oluşan kapalı devre bir sistem oluşturulmuştur. 20 mm açıklığındaki sprey odasına, soğutucu sıvı olarak dielektrik özellikteki FC-72 sıvısı dikey olarak yukarı püskürtülmektedir. Testlerde yüksek ısı yükü sağlamak için iki adet 10 Ω ince film dirençler kullanılmıştır. 10 farklı yüzey geometrisi farklı ısı yükü ve sıvı debilerinde test edilmiştir. Deney sonuçlarına göre düz finli yapılarda, 0.4 lt/dk sıvı debisinde 130 W/cm^2 maksimum ısı akısı (40.85%

iyileştirme) elde edilmiştir.

Anahtar Kelimeler: Elektronik Soğutma, Sprey Soğutma, Genişletilmiş Yüzey, FC-72

To my family

ACKNOWLEDGMENTS

TABLE OF CONTENTS

LIST OF TABLES

TABLES

LIST OF FIGURES

LIST OF ABBREVIATIONS

A	Area (cm^2)
AE	Area Enhancement
Bo	Bond Number
CHF	Critical Heat Flux (W/cm^2)
C_p	Specific Heat (J/kgK)
$C_{p,f}$	Specific Heat of Liquid (J/kgK)
d	Diameter (m)
d_0	Spray Orifice Diameter (m)
d_{32}	Sauter Mean Diameter (SMD) (m)
g	Gravity of Acceleration (m/s^2)
Gr	Grashof Number
h	Convection Coefficient (W/m^2K)
h_{fg}	Latent Heat of Vaporization
H	Distance from Orifice to Projected Surface (m)
H_n	Distance from Orifice to Test Surface (m)
HE	Heat Flux Enhancement
Ja	Jakob Number
k	Thermal conductivity (W/mK)
L	Characteristic Length (m)
Nu	Nusselt Number
Oh	Ohnesorge Number
ΔP	Pressure Difference (Pa)
Pr	Prandtl Number

q	Heat (W)
q_r	Heat in Radial Direction (W)
q''	Heat Flux (W/cm^2)
q''_{max}	Maximum Heat Transferred (CHF) (W/cm^2)
$q''_{sub,max}$	CHF with Subcooling Effect (W/cm^2)
Q	Flow Rate (lpm)
$\overline{Q}$	Average Flow Rate (m^3/s)
$\overline{Q}''$	Average Flow Rate Flux $(m^3/m^2 s)$
r	Radius (m)
r_1	Inner Radius (m)
r_2	Outer Radius (m)
Re	Reynolds Number
Re_l	Liquid Reynolds Number
T	Temperature $(^\circ C)$
T_s	Surface Temperature $(^\circ C)$
$T_{s,1}$	Inner Surface Temperature $(^\circ C)$
$T_{s,2}$	Outer Surface Temperature $(^\circ C)$
T_{in}	Inlet Temperature $(^\circ C)$
T_{sat}	Saturation Temperature $(^\circ C)$
ΔT_{sub}	Subcooling Temperature $(^\circ C)$
ΔT_e	Excess Temperature $(^\circ C)$
U	Velocity (m/s)
We	Weber Number
We_a	Air Weber Number
We_l	Liquid Weber Number
We_{d_0}	Spray Weber Number
α	Inclination Angle of Test Surface from Normal

μ	Absolute Viscosity $(Pa \cdot s)$
μ_f	Absolute Viscosity of Liquid $(Pa \cdot s)$
ρ	Density (kg/m^3)
ρ_l	Liquid Density (kg/m^3)
ρ_g	Gas Density (kg/m^3)
ρ_v	Vapor Density (kg/m^3)
ρ_a	Air Density (kg/m^3)
σ	Surface Tension (N/m)
σ_f	Liquid Surface Tension (N/m)
θ	Spray Cone Angle

CHAPTER 1

INTRODUCTION

This chapter gives brief information on electronics cooling methods and advanced heat transfer technologies. To begin with, the specific motivation behind this work, a brief review of cooling techniques, and the objectives of this research are discussed. A detailed theory and literature on spray cooling are given in the Chapter 2.

1.1   Motivation

Within past few decades electronic industry has developed vastly. Emerging technology results in more power demand in even simple electronic devices. Besides power increase, as Gordon[1] states the main reason behind increased power densities of integrated circuits is smaller dimensions. In military applications, demand for power, and therefore power density is much higher than the demands of commercial electronics. Such as in military radar applications, power increase corresponds to better performance. Hence, the main trend in these applications is pushing the limits up to thermal failure. However, current cooling technologies like natural convection, forced convection with air or liquid have very low heat removal capacities depending on the application.

1.2   Cooling Techniques of Electronics

Heat transfer phenomenon in electronics is depended on thermal energy transport to the surroundings or sink via conduction, convection and radiation. Since thermal re-

sistance in convection is much higher than conduction and radiation, convection rules the cooling mechanism [2]. For high power electronics cooling. the most widely used technique is forced convection. For less power consuming devices natural convection is preferred due to its simplicity and reliability. Theoretical heat transfer coefficient values are compared in the Figure 1.1.
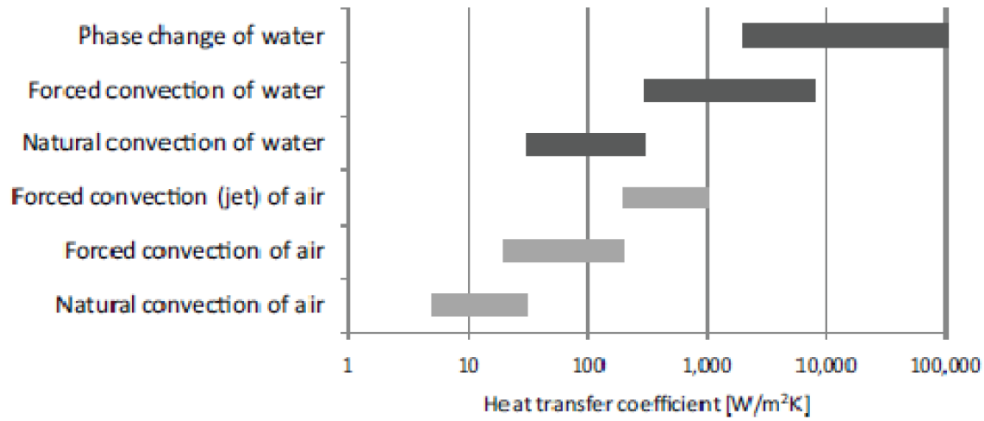
Figure 1.1: Theoretical heat transfer coefficient values [3]

Figure 1.1 shows that convection coefficient values have wide range. Depending on application, it is possible to cool very high power electronics with air or liquid according to these theoretical values. Due to limitations such as temperature gradient, size and reliability, it is not possible to reach these values for either air or water for specific applications. Using liquids in cooling systems other than air increases the heat carrying capacity.

Today's electronics are cooled with air mostly. Natural convection of air is the most common used cooling technique due to its simplicity and reliability. Performance of the cooling with convection is quantified by Newton's law of cooling which is,

$$Q = h_c A_s \Delta T \tag{1.1}$$

In Equation 1.1, there are two important parameters which is directly related to the cooling performance. Area of heat transfer surface, A_s, and the convective heat transfer coefficient, h_c determines cooling capacity. As heat transfer area increases amount

2

of heat removed from surface increases linearly which is the simplest way to improve performance. The heat transfer coefficient for natural convection is defined as [4],

$$h_c = \frac{k}{L}(Pr \cdot Gr)^n \qquad (1.2)$$

where, k is the thermal conductivity of the fluid, L is the length of the surface, Pr is the Prandtl Number and Gr is the Grashof Number. Apparently k and Pr is the material property and L is the geometrical factor. The most important value in Equation 1.2 is the Grashof Number which is defined as the ratio of the buoyant and viscous forces. This number is directly related with the surface geometry, fluid properties and temperature difference between fluid and surface. In natural convection, parameters are very few which are explained above. Hence, fluid type and area enhancement plays important role in improving cooling performance.
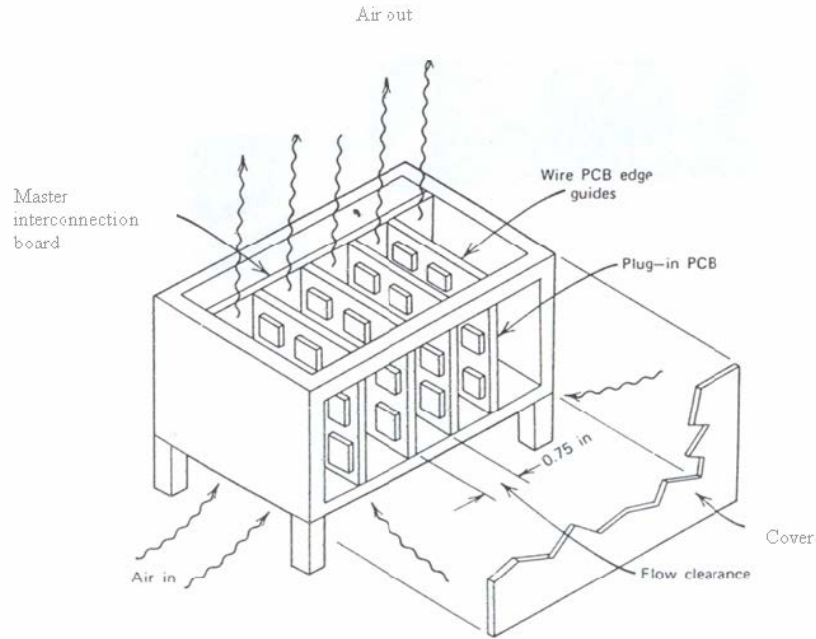
Figure 1.2: Example of natural convection heat transfer over PCBs

Nowadays, most of the electronics such as TVs, smartphones, some integrated circuits in such devices are cooled by natural convection. Reliability of natural convection makes it first choice for consumer electronics. Various fin geometries are used to increase heat transfer from the surface. However, with several hot spots on devices, limited heat carrying capacity is the biggest issue. Maximum heat flux obtained with

natural convection in such devices is only 0.05 W/cm^2 [5]. In other words, thermal resistance is very high in natural convection technique. Since area enhancement is not possible for all devices, improvement in convection mainly depends on heat transfer coefficient value.

There are several methods to increase the efficiency of convection. Recent technologies such as heat spreaders, and thermoelectric coolers make natural convection possible at higher heat flux values by reducing thermal resistance at hotspots.

Thermoelectric cooler uses Peltier effect which creates temperature difference between two sides when voltage is applied. In Figure 1.3, a schematic of thermoelectric cooler application can be seen. Heat source is placed to the cold surface while hot side is equipped with a heat sink. Cold side temperature of the thermoelectric coolers can be lower than ambient temperature which allows higher heat flux values at the source. However, as a disadvantage, these coolers have very low coefficient of performance (COP) values, meaning higher power is needed for cooling than heat dissipated [6].
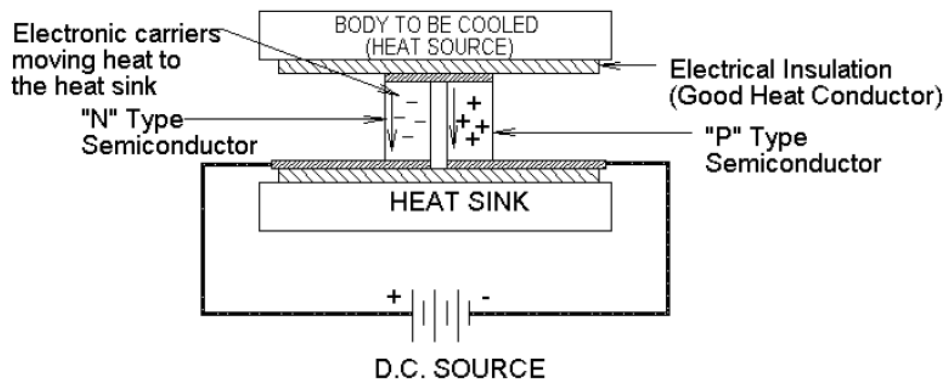
Figure 1.3: Typical thermoelectric cooler application [7]

For better cooling performance in natural convection heat spreaders are used. Materials with high thermal conductivity and heat pipes are used for this purpose. Since heat transfer area is very limited in devices, using heat spreaders helps to carry heat load to larger area with very low thermal resistance. Generally heat pipes are used in commercial products like computers, heat exchangers, etc. In fact, high heat conduction in heat pipes is achieved with phase change process. An example of heat sink - heat pipe assembly is given in the Figure 1.4.

4

Figure 1.4: Heat pipe assembly [8]

Other than heat pipes, some advanced materials are used as a heat spreaders. Carbon based pyrolytic graphite and diamond are well known spreaders. TPG, thermal pyrolytic graphite, is a unique form of pyrolytic graphite manufactured from thermal decomposition of hydrocarbon gas in a high temperature which is known as chemical vapor deposition technique (CVD). TPG core is encapsulated in aluminum or copper which makes it an anisotropic composite material with a planar thermal conductivity of 1500 W/mK. An aluminum plate with TPG can be seen in the Figure 1.5.

Unlike pyrolytic graphite, diamond is an isotropic material. Thermal conductivity values can reach up to 2000 W/mK which is 10 times of aluminum. High thermal conductivity allows low thermal gradient in high power devices while making heat sinks more efficient [9]. Usage of diamond is represented in the Figure 1.6. These techniques are mainly used in high-power RF devices, optoelectronics (Laser diodes, high brightness LEDs).
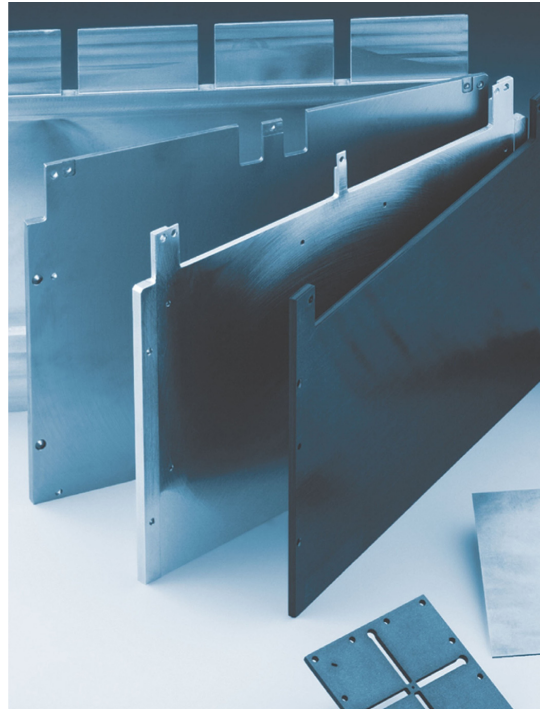
Figure 1.5: TPG (thermal pyrolytic graphite) plate [8]
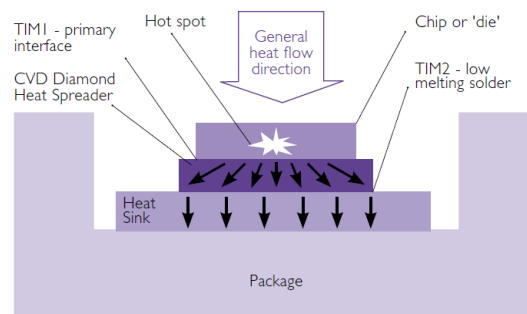
Figure 1.6: Example of diamond application [9]

Above mentioned methods have very limited usage with natural convection although they have significant improvements on cooling performance. When the limits of these devices are reached, forced convection is inevitable.

In forced convection, the movement of the fluid is accomplished by an external source. Unlike natural convection, fluid is passed over heat transfer area using fans or pumps. Nowadays, common usage of this technique can be easily observed in daily life. All computers, heat exchangers are cooled by air using fans. Since air is available everywhere and inexpensive, it is the first choice for designers. A standard fan-heat sink assembly can have a cooling capacity of 50 W/cm^2 [5]. An example of

this assembly is given in the Figure 1.7. Above mentioned enhancement techniques are also applicable for forced convection problems. Hence the efficiency of cooling can be increased by enlarging surface area or reducing thermal resistances using heat pipes, TECs, etc. Yet being an active component, fans can be seen as a drawback in cooling systems. Reliability issues and high acoustical noise are major disadvantages of fans.

Figure 1.7: Typical CPU cooler [10]

Other than conventional fans, air movement is accomplished by using piezoelectric fans or ionic driven airflow. These techniques are mainly restricted to localized cooling. Minimal noise and low power consumption are the most important advantages of these techniques. However, the maximum heat flux that can be obtained is 40 W/cm^2 and this values is lower than the heat flux of conventional fans [11].

As depicted in the Figure 1.1, as the limit of air cooling is reached, next step is liquid cooling. Although the physics of air and liquid cooling are the same, liquid cooling systems are much more complicated. An example of liquid cooling system with refrigeration cycle is given in the Figure 1.8.

Since liquids, especially water, have a great heat carrying capacity over the air, they are the first choice for cooling high power electronics. However, when using liquids in electronics there are key points to consider. As mentioned before, the design of a
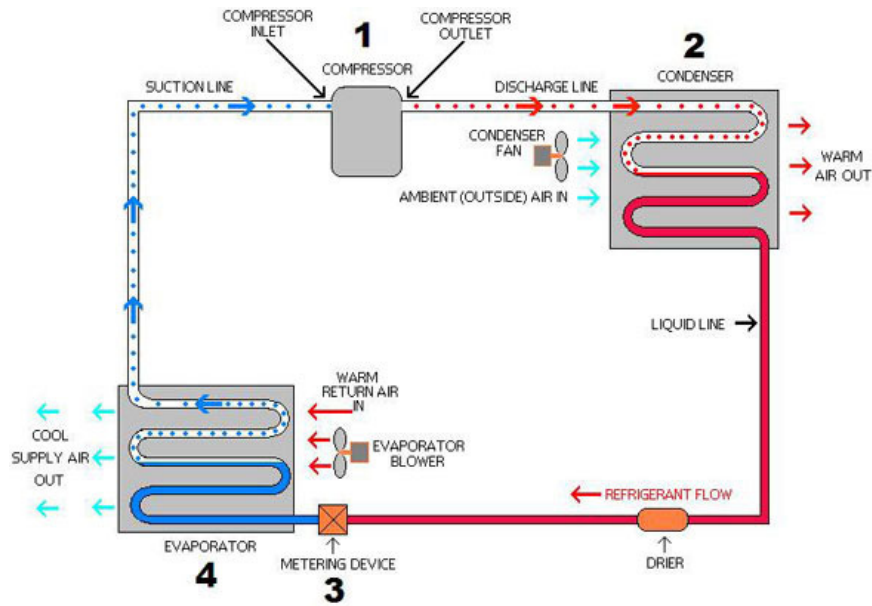
Figure 1.8: An example of liquid cooling system with refrigeration cycle [10]

liquid cooling system is complicated. Type of cooling, coolant fluid, power require-
ment and interfaces with environment are the major parameters that determine the
size of the system. Liquid cooling can be classified in two types, direct and indirect
which is depicted in the Figure 1.10.
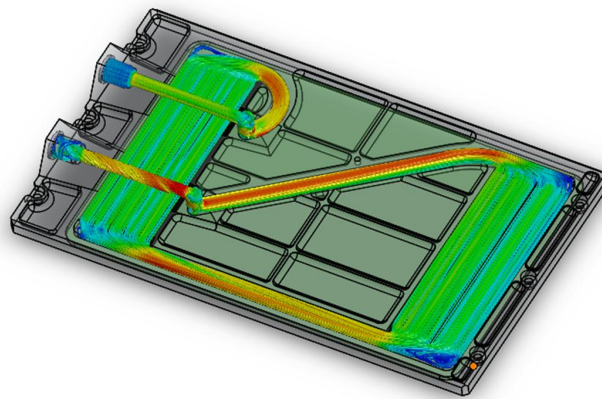
Figure 1.9: Cold plate flow visualization [12]

In direct cooling, electronics have full contact with coolant which reduces thermal
resistances caused by air and conduction path. Whereas in indirect cooling, liquid
does not contact with electronics. In such cases, cooling is provided by using cold
plates that supplies good thermal conduction path which is shown in the Figure 1.9.

With increasing heat loads, this technique is highly dependent to flow considerations. Cooling performance can be altered by increasing the flow rate but increased pressure drop results in excess pumping power.
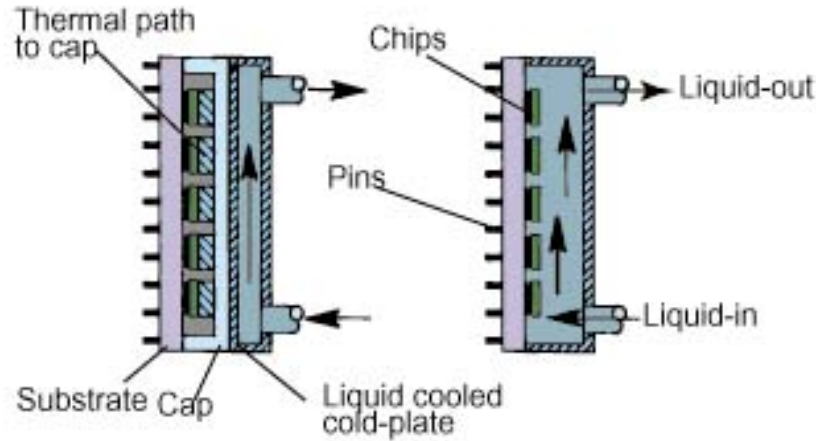
Figure 1.10: Indirect and direct liquid cooling for a chip module [10]

Type of the fluid is also important for liquid cooling systems. There is a always risk of leakage in the system when using liquids. If any leakage have a contact with heated electronics part, short circuits and unrecoverable damages can occur when a thermally conductive fluid is used. Water, glycol and alcohols, which are conductive fluids, are used as coolants fluid mostly because of their high heat cooling capacity. However, due to leakage and corrosion risks, usage of these liquids is useless for specific systems. When speaking of reliability, especially for military electronics, liquid cooling systems need much more attention. The typical minimum operating temperature for military electronics is -30 °C. At this level water can not be used since its freezing point is 0 °C. Hence mixture of water and glycol-based fluids are mostly used where very low temperature limits are specified. On the other hand, pumping power requirement is increased for glycol-based fluids which have very high viscosity values at low temperatures [13].

Low temperature limit is an important issue for large number of applications. Some engineered fluids that are used recently can be counted as liquid nitrogen, perfluoro-carbons, refrigerant fluid, etc. These fluids have very low freezing temperature points that allow them to be used within admissible viscosity ranges. Reducing pumping power has a great enhancement in terms of power requirement; however, these type

9

of fluids have lower heat carrying capacity than water [13].

Moreover, perfluorocarbons, known as "Fluorinert", are dielectric fluids which have important role in liquid cooling. They are safest cooling fluids for electronic devices, in case of any leakage in the system. Besides, in some applications, dielectric fluids are used as cooling medium. In other words, electronic devices are immersed in these fluids.
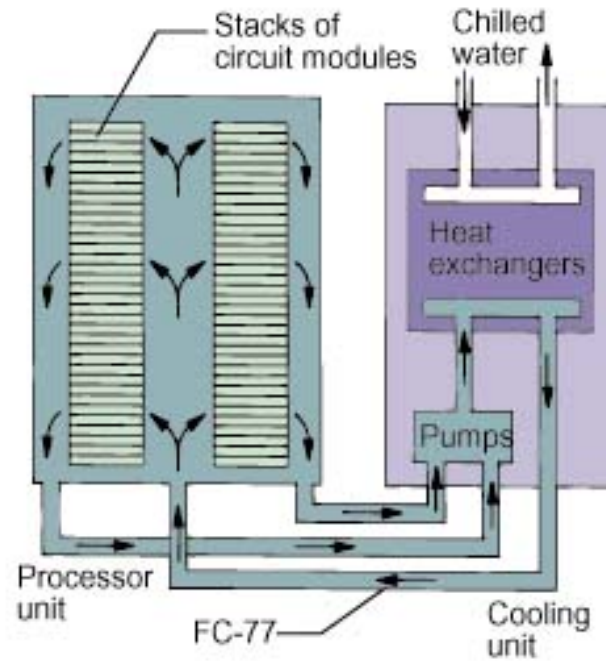
Figure 1.11: CRAY-2 liquid immersion cooling system [10]

An early application of this technique is Cray-2 supercomputer in 1985 [14] which is shown in the Figure 1.11 schematically. With low saturation point, perfluorocarbons take advantage of two-phase liquid cooling which will be discussed throughout the thesis.

Despite of high heat removal capacity of liquids, they have several limitations which are explained above. These limitations prevent achieving high cooling rates in liquid cooling. Previously mentioned improvement techniques such as heat pipes and TECs, can be applied in liquid cooling systems too. Other approaches to improve liquid cooling performance are microchannel, jet, spray and two-phase cooling.

The main goal in microchannel cooling is to increase heat transfer by increasing heat

transfer coefficient due to decreases in hydraulic diameter in the channel [15]. This technique is mainly utilized for localized, high heat flux applications. However, high pressure drop is a major drawback in microchannels.
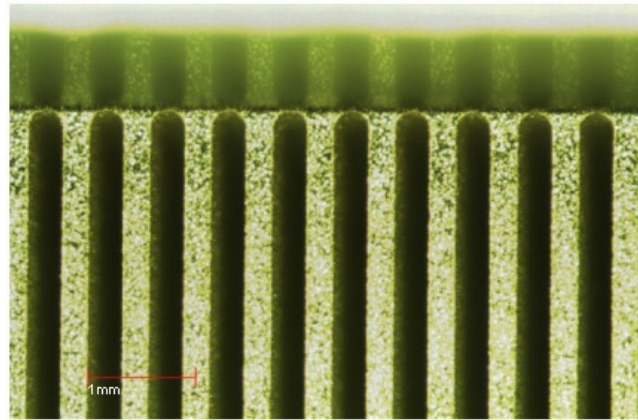
Figure 1.12: Microchannel heat sink [6]

In jet impingement cooling, heated surface is cooled by directing high velocity liquid from a nozzle normal to the surface. Impinged liquid creates stagnation point and is diverted in all directions parallel to the surface. At stagnation zone, cooling rate is high yet it decreases beyond this point. Flow pattern and example of jet cooling is given in the Figure 1.13. Although, jet cooling has a great heat removal capacity, it is utilized for very localized heat sources. Hence, for increased heated area this technique is inefficient since very high flow rates needed.
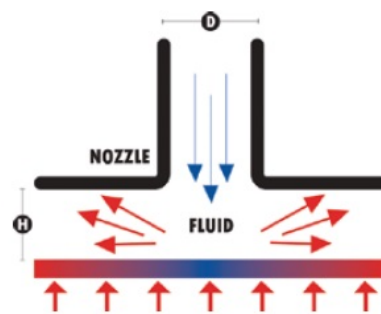
Figure 1.13: Fluid flow in jet impingement (left) Jet cooling module on PCB (right)

Two-phase cooling has the uppermost performance among all cooling techniques. Boiling is the main mechanism in two-phase cooling. At the heated surface, when temperature increases up to liquid's saturation temperature, phase change occurs and a multi-phase flow exists in the closed loop system. Major components are given in

11
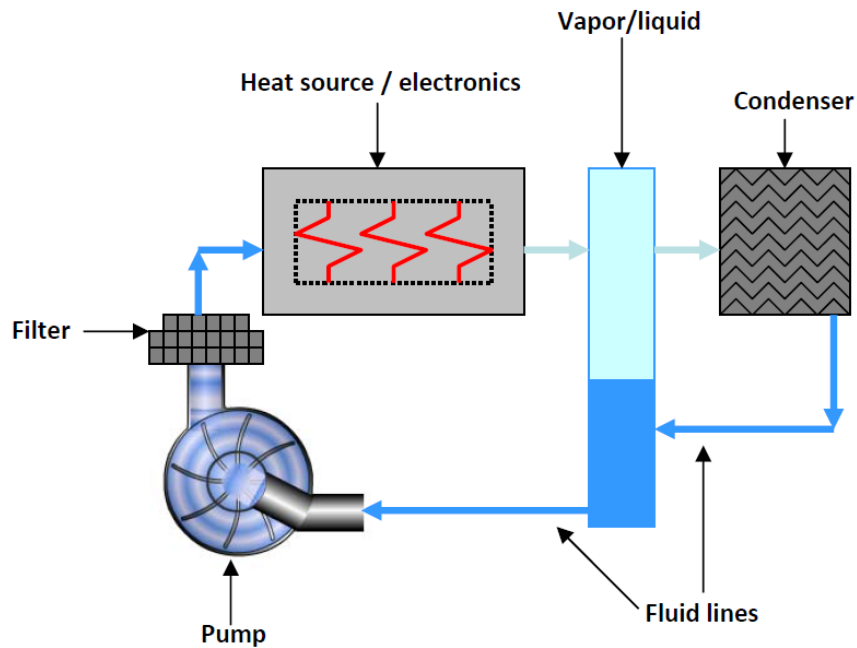
the Figure 1.14.

Figure 1.14: Major components of two-phase cooling system

The main enhancement factor is that latent heat of vaporization is utilized in two phase cooling. Two phase liquid cooling systems is that the heat of vaporization and convective benefits of boiling can increase in heat removal capacity up to 4 times when compared to single phase cooling [16]. This enhancement is not only due to latent heat but also due to buoyancy-driven bubble formation, multi phase mixing and increased turbulence on the surface.

When latent heat is utilized for cooling, isothermal cooling will be achieved. In two phase cooling very low thermal gradient occurs at saturation temperatures [16]. Performance of electronic devices, especially series of power amplifiers, are affected by non-uniform temperatures due to power derating caused by temperature difference at each amplifier [17]. Taking advantage of isothermal cooling can increase the functional reliability of these devices. All in all, to achieve high effectiveness of two-phase cooling, lower flow rates are required compared to single phase cooling. Hence, lower system flow rates result in lower pumping power requirements and much compact high heat flux cooling system. Today, two phase phenomenon in electronics cooling is observed in microchannel, jet impingement, and spray cooling. Microchannel and jet impingement cooling is mentioned as a single phase cooling

technique earlier. However, at elevated heat flux values, these systems operate at two phase regime. In two phase, using water as a coolant, maximum cooling rates for microchannel and jet impingement are increased to 275 and 1820 W/cm^2 respectively [18, 19]. Eventually, there are some additions to the system considering single to two phase transition process to handle two phase flow.

Although, spray cooling can also be used in single phase, efficiency of cooling is lower with single phase. Spray cooling can be designed to cool local hot spots with direct or indirect cooling. In direct spray cooling, dielectric fluid is impinged to bare component which is shown in the Figure 1.15. Any thermal resistance due to conduction path is eliminated with this technique. Depending on heat flux, continuous boiling occurs on the surface of component. Besides utilization of latent heat, heat transfer area is increased vastly by droplets which enhance the cooling rate.
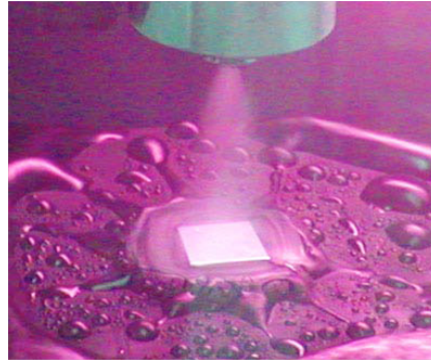
Figure 1.15: Spray cooling on a chip
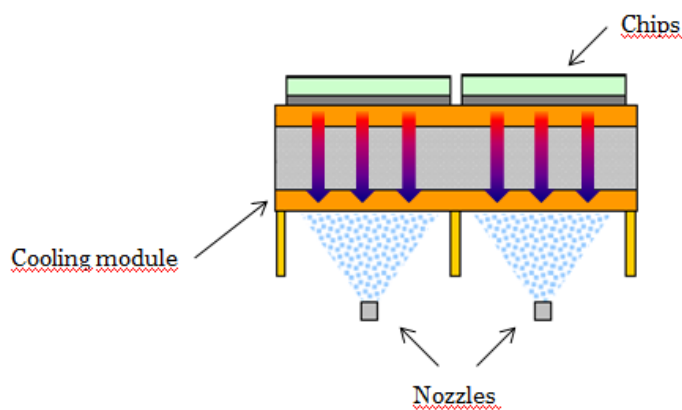
Figure 1.16: Indirect spray cooling module on a chip [20]

13

Although thermal resistances exist in indirect spray cooling, it is still advantageous. If sealing of electronics is unavoidable and non-dielectric fluids are used as a coolant, indirect spraying should be used. Same system is used in this type of spray cooling but fluid is sprayed to the heated zone. Schematic of indirect spray cooling is illustrated in the Figure 1.16.

To sum up Yan et al.[21] summarized all cooling techniques used in electronic devices with respect to maximum cooling capacity in the Table 1.1.

Table 1.1: Maximum values achieved with various cooling methods [22]

Mechanism	Cooling Method	Convection Coefficient W/m^{2}K	Heat Flux W/cm^2	Reference
Single Phase	Natural Convection of Air	5 - 25	15	Mudawar[23], Azar[24]
Single Phase	Forced Convection with Fan	10 - 250	35	Mudawar[23]
Single Phase	Natural Convection of FC	1,000	0,1 - 3	Anderson et al.[25]
Single Phase	Natural Convection of Water	800 - 2,000	5 - 90	Mudawar[23]
Two Phase	Heat Pipe	-	250	Zuo et al.[26]
Single Phase	Microchannel	-	790	Tuckerman et al.[27]
Electrical	TEC	-	125	Riffat et al.[28]
Two Phase	Pool Boiling of Water	37,000	140	Rainey et al.[29]
Two Phase	Subcooled Flow Boiling of Water	20,000	129	Sturgis and Mudawar[30]
Two Phase	Microchannel Boiling of Water	100,000 - 200,000	275	Faulkner et al.[31]
Two Phase	Spray Cooling of Water	200,000 - 400,000	1200	Pais et al.[18]
Two Phase	Jet Impingement of Water	280,000	1820	Overholt et al.[19]

1.3   Goal of the Study

As explained in "Cooling Techniques of Electronics" there are too much parameters and limitations to select appropriate cooling system for high heat flux application. Excess temperatures and thermal gradient on electronic devices are the main limitations. Most of the components can not exceed junction temperature of 150 °C; however, it is desirable to keep them at least around 100 °C since the most of the electronics undergo power de-rating at high temperatures. Moreover, performance of the devices are very susceptible to high thermal gradients. Best performance is achieved with an isothermal gradient in certain applications. In the light of these outcomes, spray cooling is advantageous among other methods for high heat flux applications, with following advantages,

- High heat flux cooling capacity

- Isothermal cooling surface

- Reduced pumping power with low flow rates

- Compactness

The aim of this work is to improve spray cooling in an applicable use in electronic devices with high heat flux. Recent works in this phenomenon are mainly limited to only experimental purpose which are not applicable in everyday applications. This study will provide an understanding on the basics of heat transfer in spray cooling and design of a simple, reliable and much more efficient spray cooling method for electronic devices. For this purpose, simple and application oriented test setup is constructed. In this test setup, ten different extended surfaces are designed for improvement of indirect spray cooling at high heat flux values. Although spray cooling has many parameters for enhancement (spray, fluid properties etc.), changes in surface properties are the simplest and the most efficient way to increase heat transfer. Performance of these extended surfaces are measured at different flow rates using FC-72 dielectric fluid. Maximum surface temperature of 100 $°C$ and heat flux of 140 W/cm^2 is aimed with a compact cooling system.

CHAPTER 2

THEORY AND LITERATURE REVIEW OF SPRAY COOLING

In this chapter, general information about flow and heat transfer theory of spray cooling is given. Spray cooling enhancement studies in the literature are explained at the end of the chapter.

2.1 Spray Mechanism

Spray is generated by a nozzle which atomizes the fluid. In atomization, stream of liquid is divided into smaller, separate fluid particles by a nozzle. Nozzles are used widely in different industrial areas. For each application, there are a variety of nozzles. The methods of atomizing can be a simple or very complex design. There are various atomizer types but pressure and gas assisted atomizing nozzles are used in the literature mostly.

Pressure atomized nozzles are the simplest nozzles among all types. Spray is generated by the swirling motion. Liquid jet is passed through a swirl chamber of grooved orifice inside the nozzle. Droplets are generated at the exit of nozzle by increased turbulence of liquid due to swirling motion. Different shapes of spray can be created by pressure atomizer nozzles. Hollow cone, circular, square, oval and flat sprays can be generated. Small sizes can be achieved by using these nozzles. For larger systems, series of atomizers are used.

Gas assisted atomizers use atomizing gas, mostly air, to produce droplets. High pressure gas is directed to the exit of liquid stream which is passed through an orifice.

This type of atomizers create finer droplets compared to pressure atomizers. Droplet diameters of 10 - 30 μm can be generated by gas assisted atomizers while it is 20 - 200 μm for pressure atomizers[32]. However presence of secondary fluid adds complexity to the closed system.

There are other types of atomizers in the literature. Rotary, acoustic, ultrasonic, electrostatic and pulsary atomizers are some of these special atomizers. However in electronics cooling these type of atomizers are not used due to their complex mechanism. They are mostly used in combustion, painting, printing, etc. applications. As a special atomizer, thermal ink-jet (TIJ) sprayers have been utilized in electronics cooling. Patel et al. [33] used TIJs to cool array of chips.

Droplet sizes of sprays are measured with Laser Doppler Anemometer (LDA) or Phase Doppler Anemometer (PDA). Nevertheless, visualization can not be possible for all applications. Therefore, an estimate parameter for characterization of various sprays are suggested by Estes and Mudawar [34] which is Sauter Mean Diameter. Sauter Mean Diameter, d_{32}, is simply an average of droplet size, namely the droplet diameter with the same volume surface area ratio as the whole spray. Sauter Mean Diameter correlation for FC-72, FC-87, and water is given in the Equation 2.1

$$\frac{d_{32}}{d_0} = 3.67 \Big[We_{d_0}^{1/2} Re_{d_0} \Big]^{-0.259} \tag{2.1}$$

where Weber and Reynolds numbers are,

$$We_{d_0} = \frac{\rho_a (2\Delta P / \rho_f) d_0}{\sigma_f} \tag{2.2}$$

$$Re_{d_0} = \frac{\rho_f (2\Delta P / \rho_f)^{1/2} d_0}{\mu_f} \tag{2.3}$$

Atomization affects the distribution of droplet velocities. Hence another parameter suggested by Ghodbane and Holman is droplet exit velocity [35],

$$V_0 = \Bigg[V_{tube}^2 + \frac{2\Delta P}{\rho_l} - \frac{12\sigma}{\rho_l d_{32}} \Bigg]^{1/2} \tag{2.4}$$

Recent research by Chen has investigated the effect of droplet size and velocity on spray cooling performance. 20 different nozzles are tested and study has showed that heat transfer coefficient and heat flux values increases as mean droplet velocity increases. However, it is also concluded that Suater mean diameter has a little effect in spray cooling performance. The possible reason is that in Equation 2.4, pressure term is dominant for pressure atomized nozzles [36].

As seen in above equations, Weber number, We, is a key parameter. Weber number is defined as fluid's inertia compared to its surface tension which is given in the Equation 2.5. This parameter plays an important role in the fluid breakup mechanism.

$$We = \frac{\rho V_0^2 L}{\sigma} \quad (2.5)$$

As depicted in the Figure 2.1, as Weber number increases, finer droplets are produced at the surface. Hence, increase in liquid velocity enhances atomization performance greatly.
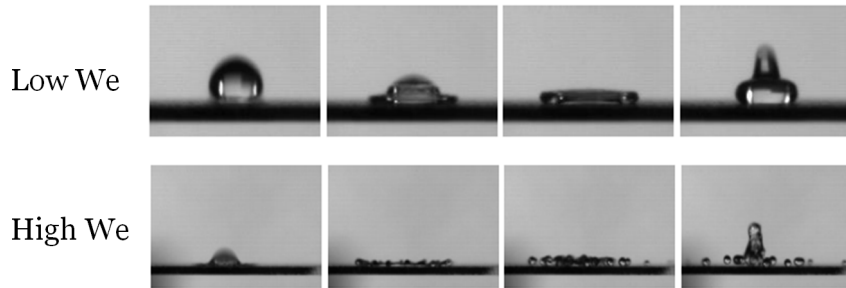
Figure 2.1: Droplet impact characteristics for low and high Weber number [37]

2.2 Heat Transfer in Spray Cooling

Single droplet studies have provided sufficient information about heat transfer mechanism in droplets. Nevertheless, multi-droplet in spray cooling makes heat transfer phenomenon very complex. When spray is generated, droplets form a liquid film on the surface. These droplets spread, scatter, splash and rebound so that flow is irreg-

19

ular. Heat transfer occurs by boiling and evaporation on this liquid film with vapor bubbles which are entrained by droplets.

Boiling is the main mechanism in spray cooling. In boiling, there are both single and multi-phase heat transfer. Sensible and latent heating are utilized in boiling. In Figure 2.2 typical boiling curve with certain regimes is given.
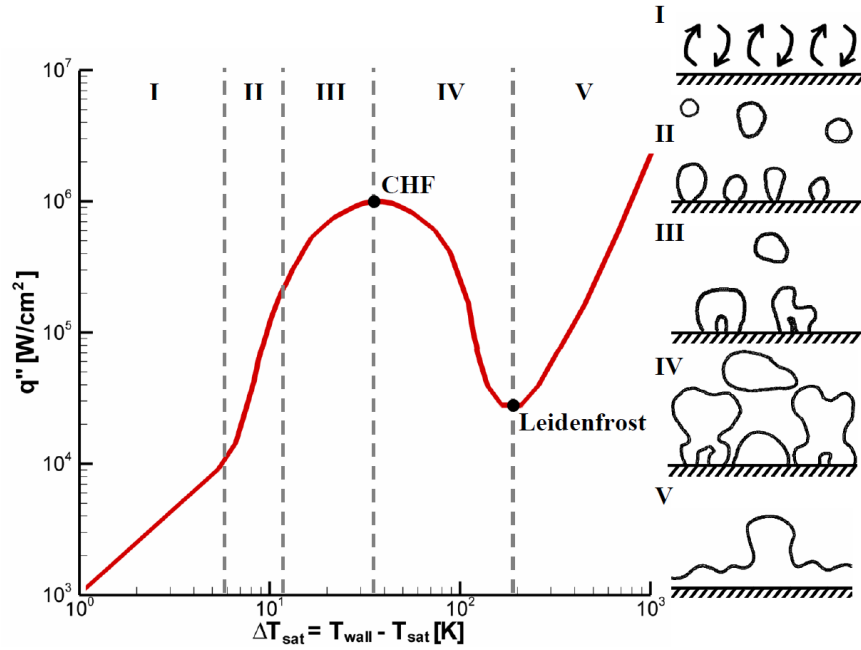
Figure 2.2: Typical boiling curve [38]

The first region is defined as free convection boiling. Very low temperature difference ($\approx 5°C$) occurs in single phase regime. Thus very low heat flux is observed. No nucleation starts until the end of this region. Then, in the second region which is called nucleate boiling regime, nucleation starts. There is a transition process from single phase to multi phase heat transfer. With increasing temperature difference, frequency of bubble generation increases exponentially. Hence a sharp rise in heat flux is observed. Heat flux continues to increase with decreasing rate up to critical heat flux (CHF) point. Droplets cannot reach the heated surface since rate of nucleation reaches maximum. Hence insufficient liquid supply results in dry-out on the surface. After reaching local maximum heat flux, transition region starts. In this unstable region, dry surfaces are increasing which results in decrease in heat flux down to Leidenfrost point. At this point, the surface is fully covered by vapor film. After that, in the fifth region film boiling starts in which heat transfer occurs by conduction and radiation

20

through the vapor film.
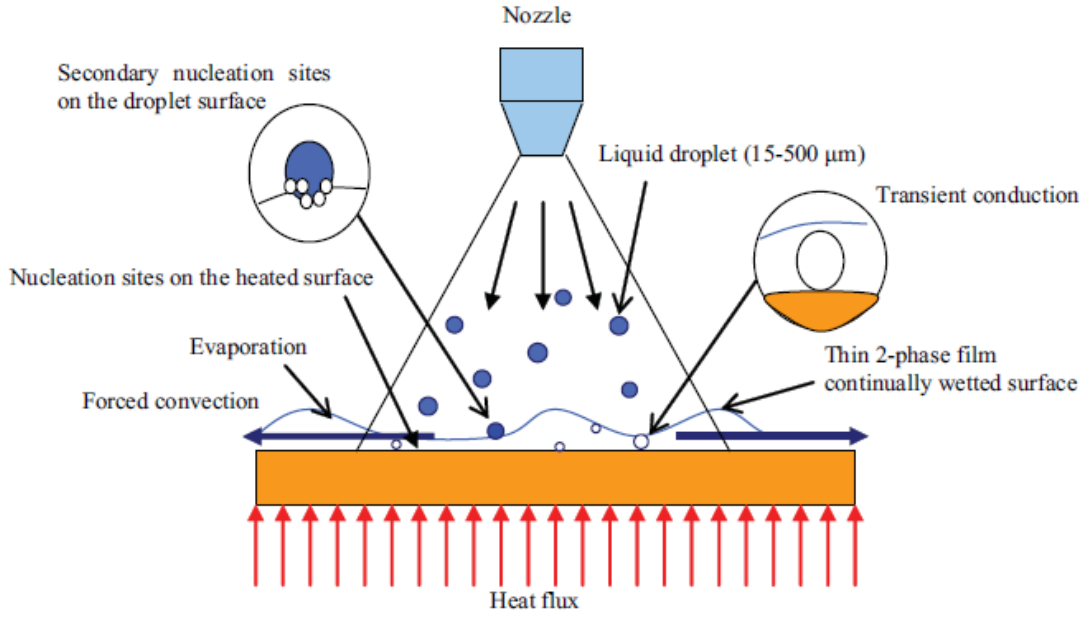
Figure 2.3: Illustration of spray on heated surface [21]

Spray cooling curve is the same as the first three regions of boiling curve. Spray cooling process is depicted in the Figure 2.3. Nucleation, intense convection and secondary nucleation are observed mechanisms in the spray cooling. At single phase region, forced convection is the main heat transfer mechanism. When nucleation is initiated two-phase regime starts in spray cooling. Yang et al.and Rini et al. observed that boiling is enhanced by secondary nucleation which is defined as added nucleation sites due to impinging droplets entrain vapor bubbles in liquid film [39, 40]. At this stage, nucleation and transient conduction in the liquid film with latent heat transfer enhance cooling rate up to CHF point. Generally spray cooling application is limited to CHF point in the view of fact that CHF is highly unstable point for a safe operation for electronics. However, especially in metal quenching applications spray cooling is utilized at film boiling region [41].

Since the maximum heat transfer is obtained at CHF point, for spray cooling applications, spray cooling efficiency is defined as, the ratio of the CHF to the heat transfer capability of the fluid,

$$\eta = \frac{\dot{q}''_{CHF}}{\dot{m}'' \left[c_{p,l} \left(T_{sat} - T_{fluid} \right) + h_{fg} + c_{p,v} \left(T_{wall} - T_{sat} \right) \right]} \quad (2.6)$$

21

which is the thermodynamical limits of sensible, latent and vapor heat transfer. Though, vapor heat transfer terms are generally neglected. It should be noted that in this equation, although the heat transfer increases with mass flux, spray efficiency generally decreases in spray applications [42].

2.2.1 Spray Cooling Correlations

Although its mechanism is not well understood, there are several spray cooling correlations in the literature. First correlation by Ghodbane [35] and Holman [43] is given as,

$$\frac{q''x}{\mu_l h_{fg}} = 9.5(We)^{0.6} \left(\frac{c_{p,l}\Delta T}{h_{fg}} \right)^{1/2} \tag{2.7}$$

The heat flux is correlated as a function of nozzle distance "x" which was 19 cm for this experiment. Freon-113 is used as a coolant fluid. Droplet velocities and diameters varied from 5.4 to 28 m/s and from 210 to 980 μm, respectively. In the experiments maximum heat flux was reported as about 25 W/cm^2.

Another correlation is suggested by Rybicki and Mudawar [44]. In the experiments, PF-5052 was used. They also used the water spray data of Mudawar and Valentine to get the following correlation [45],

$$q'' = 4.70 \frac{k_l (T_{wall} - T_{inlet})}{d_{32}} \left(\frac{\rho_l \bar{Q}'' d_{32}}{\mu_l} \right)^{0.61} (\mathrm{Pr}_l)^{0.32} \tag{2.8}$$

However, it should be noted, the developed correlation is in single-phase only. The mean absolute error was 13.1% based on experimental data.

Later a correlation is developed for the heat transfer coefficient. Shedd and Pautsch developed the following correlation based on energy transfer [46],

$$h = 0.4627 \rho_l c_{p,l} \bar{Q}'' + 0.01612 \bar{Q}'' \Delta T_{sat} \tag{2.9}$$

For single nozzle studies, sensible heat contribution is superposed with a two-phase contribution linearly. Later another correlation was developed for multiple nozzle array. However, this correlation is limited in terms of heater area, flow rates and thermophysical properties of different fluids.

Although there are few empirical heat flux predictions for spray cooling applications in the literature due to its complicated nature, Estes and Mudawar have a good prediction on CHF with "Volumetric Flux Model (VFM)" [34]. FC-72 and FC-87 dielectric fluids were used in the experiments. It was found that if nozzle was placed close to heated surface, the spray impact area got smaller and only a small fraction of the heater area was utilized, resulting in low CHF values. CHF was increased as the distance between nozzle and surface was increased. Maximum value was observed when the spray cone fully covered the whole heated surface. At higher nozzle-surface distances, it was observed that CHF values decreased. Correlation is given as,

$$\frac{q_m''}{\rho_g h_{fg} \overline{Q}''} = 2.3 \left(\frac{\rho_f}{\rho_g}\right)^{0.3} \left(\frac{\rho_f \overline{Q}''^2 d_{32}}{\sigma}\right)^{-0.35} \left(1 + 0.0019 \frac{\rho_f C_{p,f} \Delta T_{sub}}{\rho_g h_{fg}}\right) \left(\frac{f_1^{0.30}}{f_2}\right) \quad (2.10)$$

Where f_1 and f_2 are the geometric factors which are defined as,

$$f_1 = \frac{1}{8}\left(\frac{L}{H}\right)^2 \frac{\cos\alpha\sqrt{1 - \tan^2\alpha\tan^2(\theta/2)}}{1 - \cos(\theta/2)} \frac{dA'}{dA} \quad (2.11)$$

$$f_2 = \frac{1}{\left[\frac{\pi}{4}\cos\alpha\sqrt{1 - \tan^2\alpha\tan^2(\theta/2)}\right]} \quad (2.12)$$

It was reported that the uncertainty was as high as 30%. This correlation is verified by numerous studies in the literature. Rybikci et al. validated this correlation for upward-oriented sprays with PF-5052 as a working fluid [44]. Besides, VFM (1995) model given in the Equation 2.10 is verified by a plenty of experiments in the literature [47]. However, in 2009 Visara and Mudawar have modified the subcooling term in VFM

from 0.0019 to 0.0050 [48]. The new correlation was given as,

$$\frac{q_m''}{\rho_g h_{fg} \overline{Q}''} = 2.3 \left(\frac{\rho_f}{\rho_g}\right)^{0.3} \left(\frac{\rho_f \overline{Q}''^2 d_{32}}{\sigma}\right)^{-0.35} \left(1 + 0.0050 \frac{\rho_f C_{p,f} \Delta T_{sub}}{\rho_g h_{fg}}\right) \left(\frac{f_1^{0.30}}{f_2}\right) \quad (2.13)$$

Other than pressure atomized sprays Chow et al. (1995) developed CHF correlation for air-atomizing sprays. The maximum deviation was 30% of their data.

$$\frac{q''_{CHF}}{\rho_l \overline{Q}'' h_{fg}} = 0.38 \left(\frac{\sigma}{\rho_l \overline{Q}''^2 d_{32}}\right)^{1/3} \left(\frac{\rho_v}{\rho_l}\right)^{1/2} \left(\frac{P_s}{P_a}\right)^{1/4} \quad (2.14)$$

2.3   Previous Studies on Surface Enhancement

Surface enhancement is studied in pool boiling application primarily. Nucleate boiling can be enhanced by surface roughening or using extended surfaces in which density of nucleation sites are increased. In 1960, Kurihara and Myers studied roughness effect on nucleate boiling [49]. Increase in heat transfer was observed due to increase in nucleation site density by surface roughening. Others have extended this technique by creating porous structures on the heater surface. Nakayama et al. used microscale tunnels, pores and extended surfaces in their studies [50]. With the same heat, lower surface temperature of 80 – 90% was achieved using R-11, water, and nitrogen. Mudawar and Anderson also studied more fin-like extended surfaces using microgrooves, square microstuds, and pin fin arrays [25]. Maximum enhancement was about 159 W/cm^2 which was 8 times of plain surface.

In the light of surface enhancement on pool boiling, some enhancement mechanisms have been studied in recent years. Study by Pais et al., reported that heat flux decreases with increasing surface roughness for gas atomizing nozzles [18]. Nevertheless, liquid atomizing nozzles showed an increase in heat flux with increasing surface roughness in the work of Sehmbey et al. Lately, Sodtke and Stephan used water to cool a porous surface as well as ones with triangular microgrooves and pyramids

[51]. They found no improvement with the microporous structure. However, with microgrooves and micro pyramids they observed a 2-5 times enhancement when the superheat exceeded 6 °C and no enhancement at lower superheats. It was posited that the higher superheat ruptures the liquid film, allowing capillary forces to distribute a thin film equally between the fin troughs and tips.

Bostanci et al. conducted experiments on enhanced surfaces by using a vapor atomized spray nozzle [52]. Fluid used in the experiments was ammonia. Their test surfaces were micro-scale indentations and protrusions, macro scale pyramidal pin fins, and multi-scale fins. Maximum heat flux with multi-scale fin surfaces was 910 W/cm^2 where the enhancement was limited by 18% compared to bare surface. Best enhancement factor of 67% was obtained by combination of multi-scale structured and pyramidal fins/protrusions. Heat flux was increased to 1100 W/cm^2 with this arrangement. Authors concluded that enhanced surfaces can retain and spread more liquid via capillary force within the structures. Since the dryout was delayed further, higher CHF values could be obtained.

Similarly, in very recent paper Yang et al. demonstrates that micro-cavity surfaces have a great enhancement on spray cooling [53]. In this study, spraying surface was made of copper with a project area of 2.5 cm × 1.2 cm. Ammonia was used with multiple nozzle array. Maximum heat flux obtained was 451 W/cm^2 (1.5 times of flat surface) with an area enhancement of 163% and Bo number of 0.1004. They suggested that lower Bo number for the surface with micro-cavities should be preferred to the enhancement of spray cooling performance.

Souza and Barbosa Jr. had a different approach on surface enhancement recently [54]. Their method utilized a 5 mm high brazed copper-foam on 25 mm diameter sprayed surfaces which had 10 PPI pore density and 90% porosity. Using refrigerant R-134a fluid with single pressure atomized nozzle, experiments were conducted at two different flow rates, 3.0 and 5.0 kg/h. Results of the experiments showed that CHF value did not change for copper foam surface arrangement. However, significant increase in heat transfer coefficient was achieved with the copper-foam enhanced surface. Authors suggested that further research should be done on enhancement mechanism for foam like structures.

The most comprehensive study on extended surfaces was carried by Silk et al. PF-5060 was used under gassy (101 kPa) and degassed (41.4 kPa) chamber conditions [55]. Performance of straight fins, cubic pin fins, pyramids, dimples and porous tunnels were tested with multiple nozzle array where the bare surface area was 2 cm^2. Results showed that extended surfaces improve heat transfer performance by increasing critical heat flux (CHF). Maximum ehancement compared to flat surface was achieved by straight fins which was about 48% increase in CHF at degassed case. Study also showed that although pyramidal fins had the maximum area, they performed worse compared to other surface structures. Author suggested that this enhancement by extended surfaces could be related to liquid management on the surfaces. Silk explained this phenomenon by drainage area change on the surfaces. Straight fins had smaller drainage area in which the liquid velocity increases, resulting in higher heat transfer coefficient in the channels.

Coursey et al. performed spray cooling experiments on six straight fin structured surfaces (projected area: 1.41×1.41 cm^2) with the height varying from 0.25 to 5 mm [38]. The straight fin surfaces were fabricated with the electric discharge machined (EDM) method on a copper block heater and PF-5060 was chosen as the test fluid. It was found that the enhanced surface improves the cooling performance significantly compared to the flat surface and the longer fins outperformed shorter ones in the single phase heat transfer regime. With the flow rates up to 1.0 mL/s, there was an optimal fin height ranging from 1 to 3 mm for the high heat flux up to 124 W/cm^2.

The latest solution was presented by Xie et al. with structured surfaces in spray cooling [56]. In this study 8 different finned heater surfaces were introduced with micro-, macro- and multiscale-structured straight and square fins. Maximum area enhancement factor was 2 in all surfaces. Refrigerant R-134a fluid was atomized with six swirl nozzle array and the droplet sizes and velocities were 189 to 172 μm and 18.1 to 24.6 m/s, respectively. Experiment results showed that multiscale-structured surfaces had the maximum heat transfer enhancement of 65% where it was 32% and 36% for micro-flat and macro-structured geometry, respectively. Authors concluded that fin arrangement is much more important than wetted area increase in macro-structured surfaces. It was explained by increased velocity in drainage.

26

On the other hand, the results obtained by Lin et al. showed that CHF decreased for large area (above 2 cm^2) spray cooling when using single nozzle [57]. Experiments conducted in the literature mainly had a small heated area. Hence Lin et al. studied large area spray cooling with multiple nozzle array. The sprayed area was 2.54 $\times$ 7.6 cm^2. FC-72 was utilized as a coolant fluid and a decrease in CHF of 34% was observed. Authors suggested effective fluid management and proper design of the side channel.

CHAPTER 3

EXPERIMENTAL SETUP AND PROCEDURE

Numerous experiments were designed and constructed to study the effect of extended surfaces in spray cooling. The various experimental components, procedures, and methodologies used in these studies are described below.

3.1   Test Setup

An experimental setup is designed to test various extended surfaces using a closed fluid loop system. This liquid cooling system consists of a spraying chamber, a custom made microchannel heat exchanger which is used as a condenser unit, a gear pump, a valve, a filter and a relatively small reservoir as given in the Figure 3.1. In addition to these components, the test setup consists of heaters, heat exchanger fan, pressure and temperature transducers with a data logger and a flow meter. There are three DC power supplies for all devices in the experimental setup.

Since various experiments will be conducted with different enhanced surfaces, experimental setup is designed as simple as possible. A better and simpler view of the experimental setup can be seen in the Figure 3.2. Fluid is delivered by a DC internal gear pump manufactured by Micropump (GB P25) which can provide 840 ml/min flow rate at 1400 RPM with maximum 5 bar system pressure. Pump is powered by a DC power supply and flow rate of the pump is adjusted by changing the supply voltage of the pump.

There are flow rate, pressure and temperature sensors before the inlet of the spraying
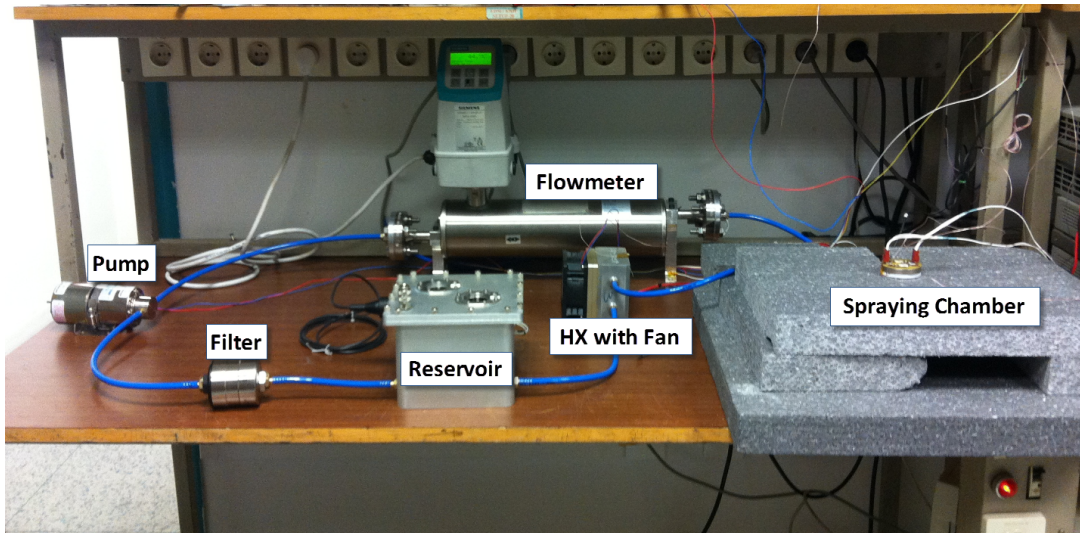
Figure 3.1: Overview of Experimental Setup

chamber. Flow rate is measured by SIEMENS SITRANS F C, which is a corriolis mass flow meter that measures the flow rate, density, inlet temperature of the liquids simultaneously.
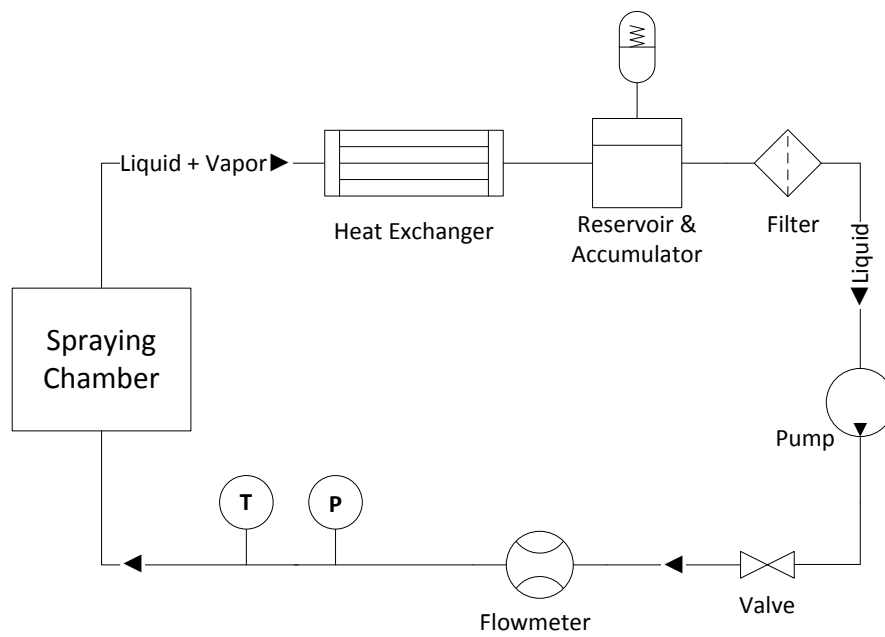
Figure 3.2: Experimental Setup for Spray Cooling

Before the inlet of the spraying chamber, pressure is measured by a miniature and rugged transducer (Kulite HKL/T-1-235) which has a maximum of 7 bar pressure

range. After spraying chamber, the fluid is passed to the heat exchanger.

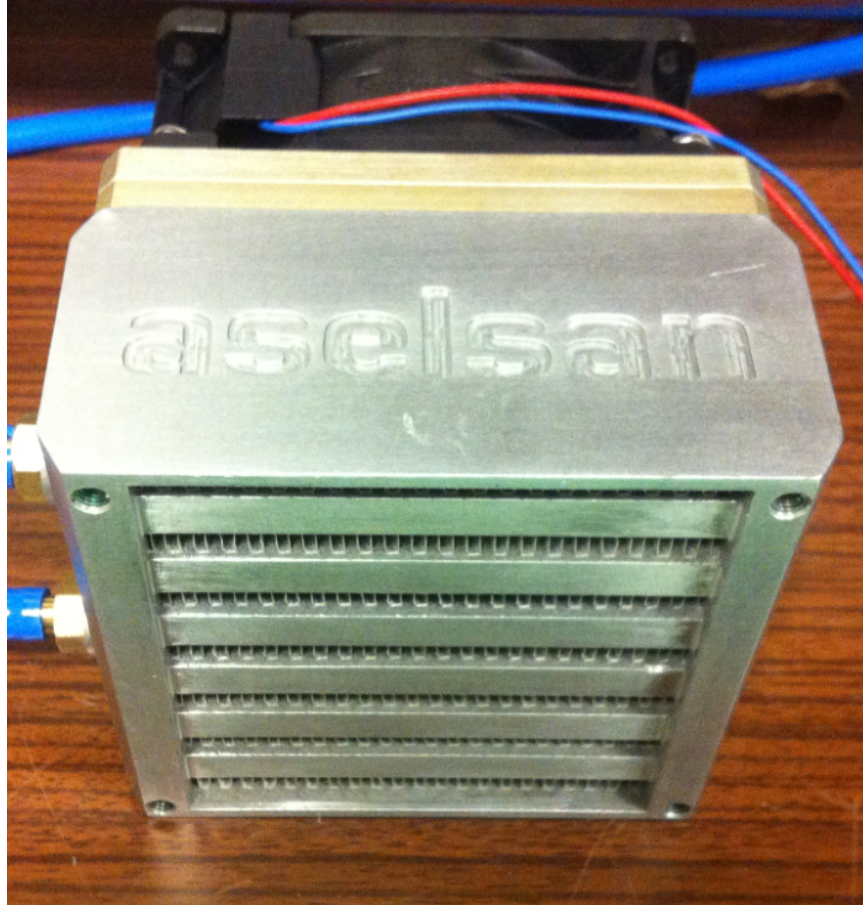The heat exchanger is a custom made, compact and high performance microchannel heat exchanger [58]. Air-cooled condenser is equipped with an axial fan (Figure3.3). The reason of a need for a high performance heat exchanger is to obtain liquid phase at the exit of the condenser.

Figure 3.3: Heat Exchanger - Fan Assembly

After heat exchanger, liquid is drawn to the reservoir which is shown in the Figure 3.4. Since main reason of this study is to get a small spraying cooling application, reservoir is kept as small as possible. It has 3-liter capacity. The size of the reservoir is important because the temperature in the reservoir should be constant during the experiments. Also another parameter in the reservoir is the system pressure. Since it is a closed liquid system, any change in the system pressure changes the spraying pressure. Thus, two edge welded bellows (Bellows Tech 0150A-034) are used to keep the pressure in the reservoir almost equal to atmospheric pressure.
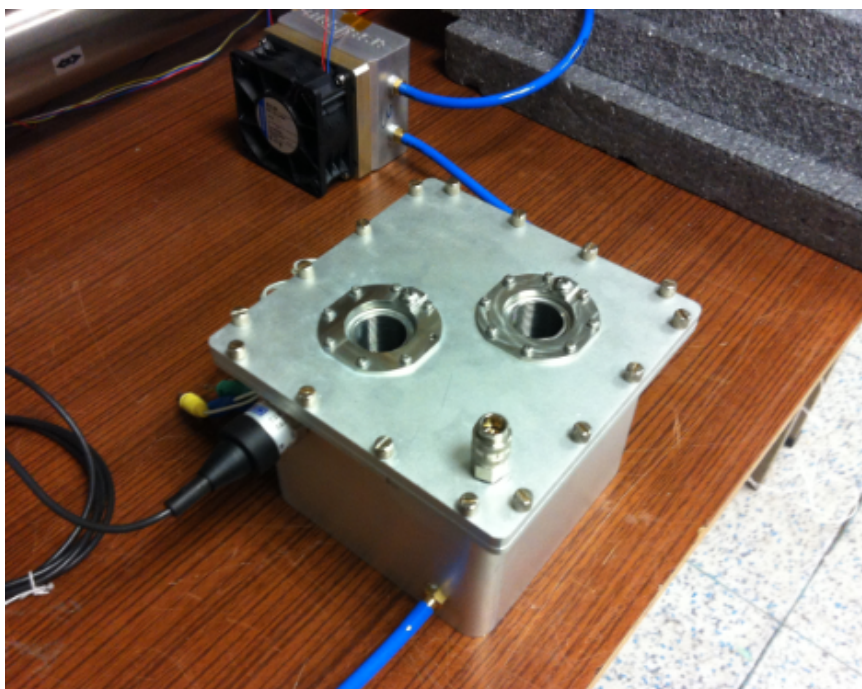
Figure 3.4: Reservoir

Although very pure and corrosion free FC-72 fluid is used in the system, there is a 50 μm filter placed at the inlet of the pump to protect spray nozzle and pump. All these components are connected via 6 mm high temperature resistant flexible plastic tube by Legris.

3.1.1 Spraying Chamber

Spraying chamber plays an important role in this setup. Chamber contains spraying cap, nozzle and heated surface. Schematic of the chamber is given in the Figure 3.5. The main goals in this study are compactness and simplicity. Thus spray cap has 20 mm opening and it is made of PTFE which is known as "Teflon". Due to its low thermal conductivity and high temperature resistance (about $200°C$ - $260°C$), Teflon is the best choice for the insulation of the spraying chamber. Chamber is designed to be as small as possible and work with different extended surfaces easily. Hence the heater is placed on the top of the spraying cap and sealed with a NBR o-ring for leakage, outgassing and ease of using different heated surfaces. As seen in the Figure 3.5, a single, pressure atomized nozzle is placed at the bottom of spray cap. A stainless steel nozzle from Spraying Systems which has minimum $53°$ spraying
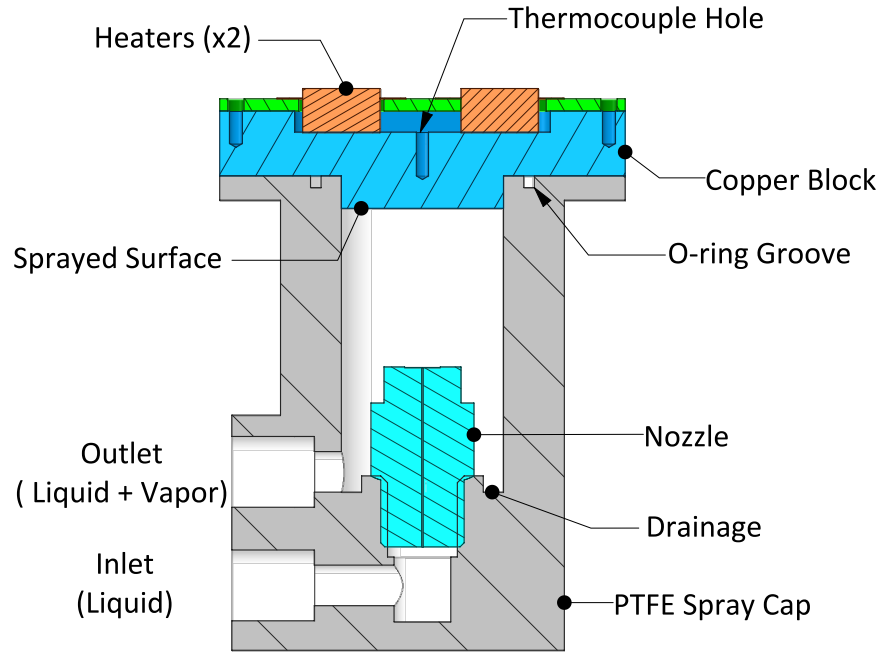
Figure 3.5: Spraying Chamber

angle with 0.762 mm orifice diameter is used. Nozzle is placed 20 mm away from the sprayed surface to ensure that the whole surface is covered by fluid. Since it is a closed system, there is no chance to visualize the flow. For that reason, sprayed surface is tested by placing PMMA screen at the top of spraying chamber before the experiments. In the Figure 3.6, it can be easily seen that whole surface is covered
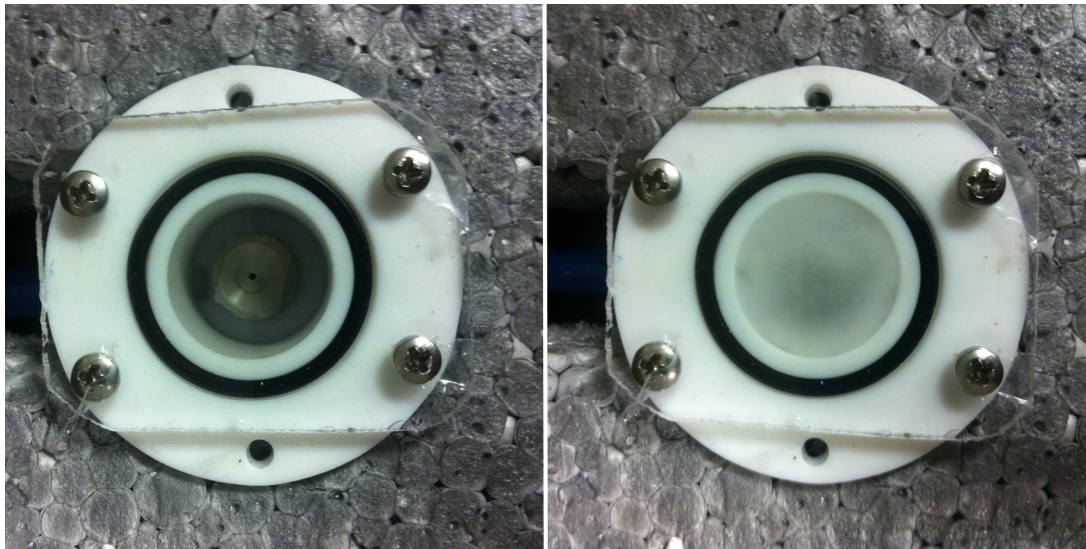
Figure 3.6: No flow (left); flow condition (right)

well. Since the fluid sprayed towards upward direction, gravity will help the returning liquid to drain well at the bottom of the chamber. During visual flow test no blockage of the flow is observed.
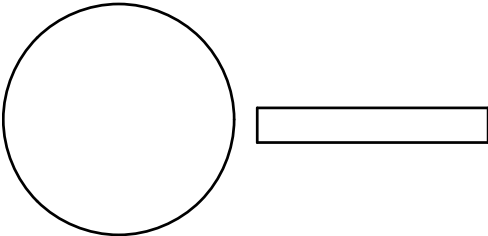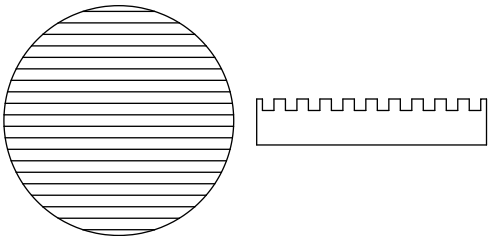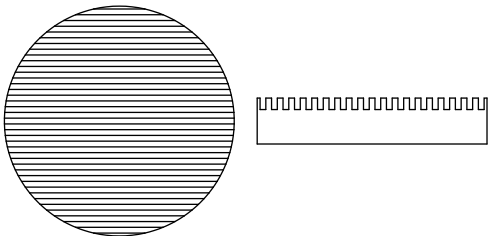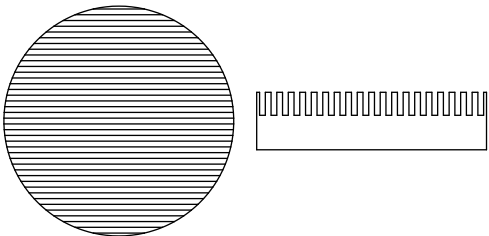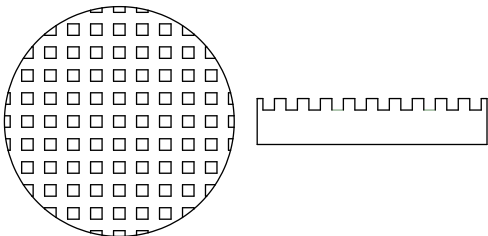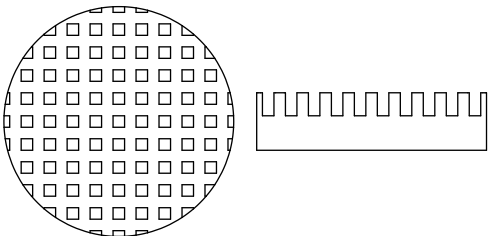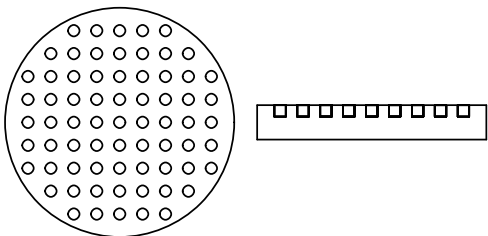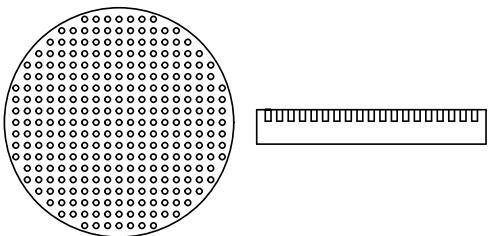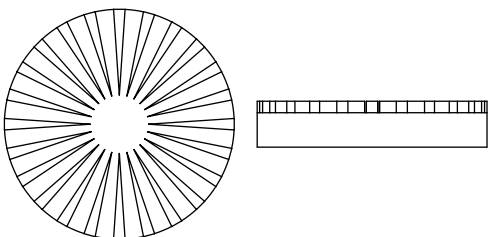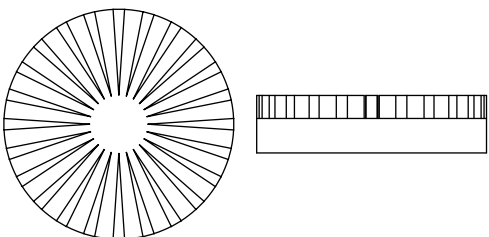
Sprayed surface with different patterns is mounted at the top of the spray chamber. Patterns used in experiments are listed in the Table 3.1 and Figure 3.7 with pattern names. Using such patterns is due to their ease of machinability and simplicity. Additionally, extended surface investigation in spray cooling is widely encountered in literature [55, 59].
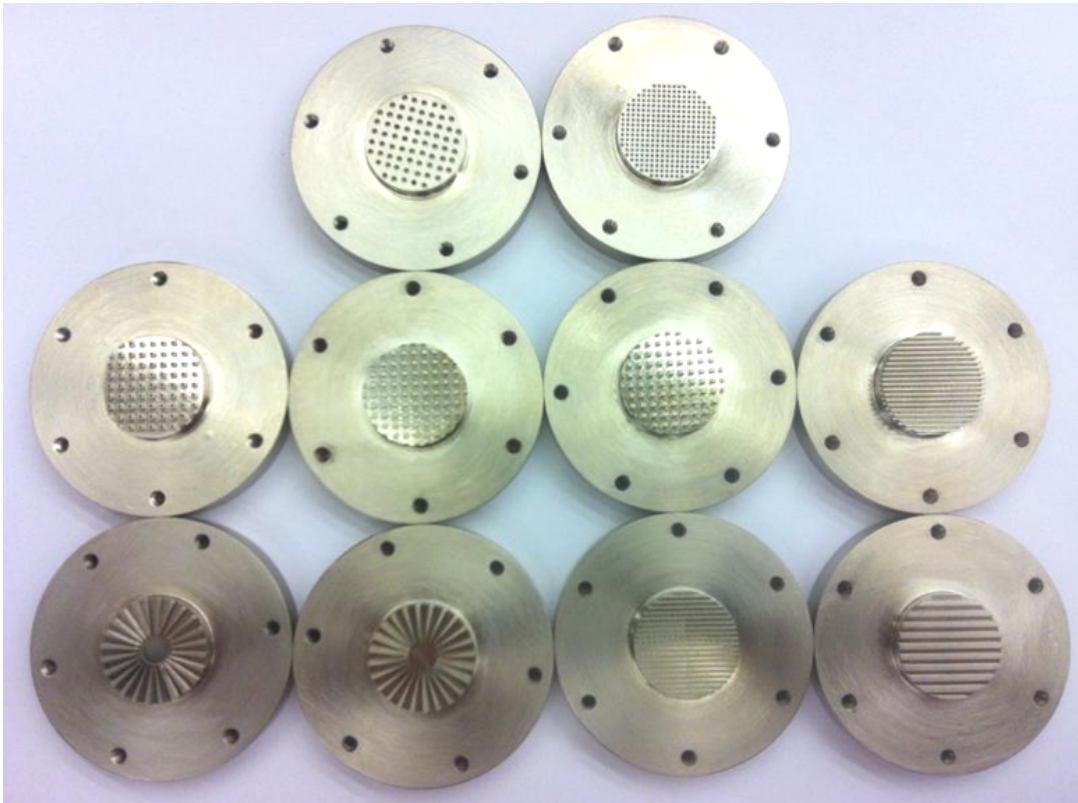
Figure 3.7: Sprayed surface patterns

Each surface is made of copper with a 5 μm nickel surface coating (Figure 3.8). Copper block has a 20 mm neck, meaning that the frontal area of the sprayed surface is 3.14 cm^2. The main reason of using copper is its low thermal resistance. To measure surface temperature, thermocouples are placed 2 mm away from the surface. With low thermal resistance of copper, measured temperature will be very close to surface temperature. There are two J-type thermocouples in a hole. For surface temperature measurements, the average of these two thermocouple readings are used. Heat loss to

Table 3.1: Sprayed Surface Geometries

Flat	Straight Fin 1
Straight Fin 2	**Straight Fin 3**
Cubic Fin 1	**Cubic Fin 2**
Holes 1	**Holes 2**
Radial Fin 1	**Radial Fin 2**

the surroundings are estimated to be low. A detailed analysis is done for heat loss in Chapter 3.3. At the bottom of copper block, PTFE spray cap provides good insulation and at top of the block, a PCB of the heaters is placed which is a good insulator too. Only the sides of the copper block are open to surroundings. The heat loss from the circumferential area is estimated with thermal analysis which will be discussed later.
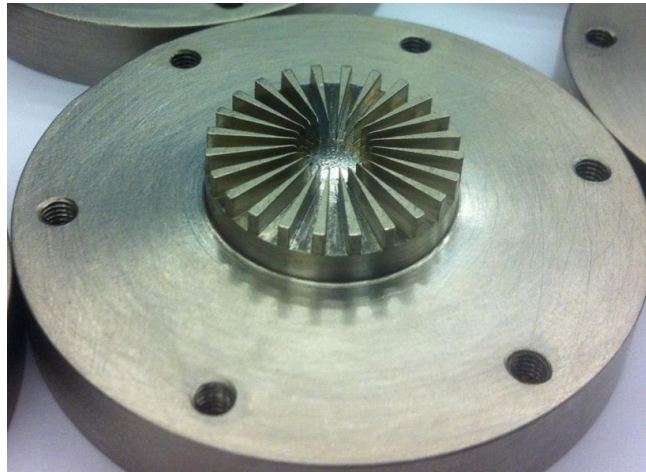
Figure 3.8: 5 μm nickel coated surface

As a heater, two flange-mounted thin film resistors from RF Florida are used for each surface. These resistors are soldered to PCB which can be seen in the Figure 3.9. The power rating of each device is 250 W maximum which means 500 W heat can be given to the system in total. Hence, maximum heat flux supplied can be about 160 W/cm^2. The maximum operating temperature of the resistors is 150°C which is also measured by a J-type thermocouple. Power applied to these resistors is controlled by 1000 W Agilent DC power supply.

All readings of sensors which are pressure and thermocouples are monitored by computer interface. Agilent 34970A data logger is used which is attached via RS-232 interface.
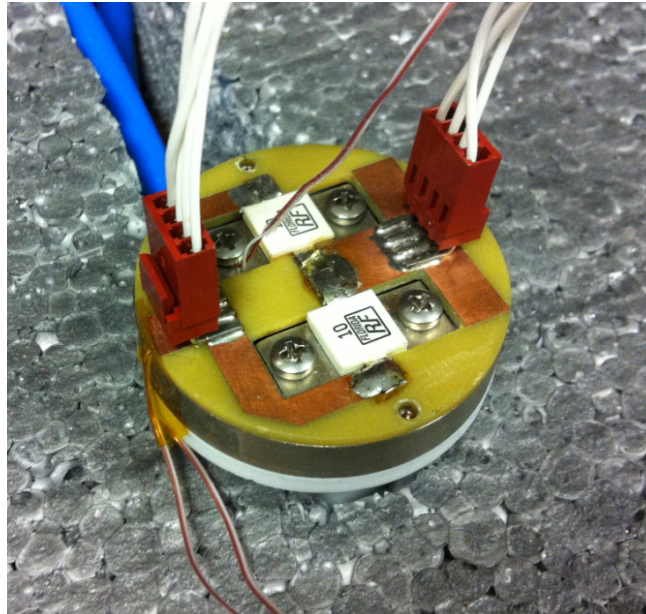
Figure 3.9: Heaters

3.2 Experimental Procedure

There are at least ten sets of experiments for different spray surfaces. A definite procedure for every set of experiments must be followed. Prior to experiments, safety precautions are taken. Electrical and fluid connections are checked before beginning of the experiments. After checking all temperature, pressure readings, switches and valves, experiment is started. In these experiments there are two controlled variables; sprayed surface and flow rate. At the beginning of each experiment one sprayed surface is selected and mounted to the spray cap. Flow rate in the system is changed by changing speed of the pump. Pressure is directly related to the flow rate. Hence pressure is also a characteristic variable in these experiments. Following chart summarizes experimental procedure for each surface,

Important points in this experimental procedure are heat input and temperature recordings. Heaters are powered by a DC power source. As first heat input for each sprayed surface, 15 VDC is applied to the heating resistors. Current output is monitored at the DC power supply. Then temperature is monitored continuously to see whether the temperature is in steady trend or not for a given heat input and flow rate. After judging steady state condition, temperature of the surface is recorded. After that heat
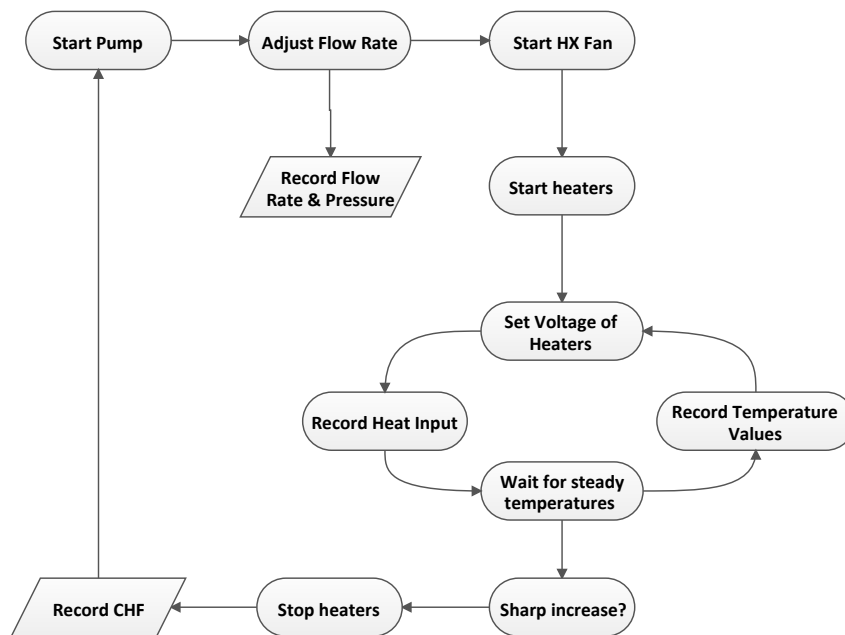
Figure 3.10: Experimental procedure

input is increased by increasing the voltage. As mentioned above, these steps are repeated until very sharp increase in temperature is observed. At this point, dry-out - critical heat flux (CHF) - occurs on the surface resulting in a sudden temperature increase. Corresponding heat flux and temperature values are recorded, which are the maximum heat flux (spraying CHF) and maximum surface temperature. Figure 3.11 demonstrates sample thermocouple readings.
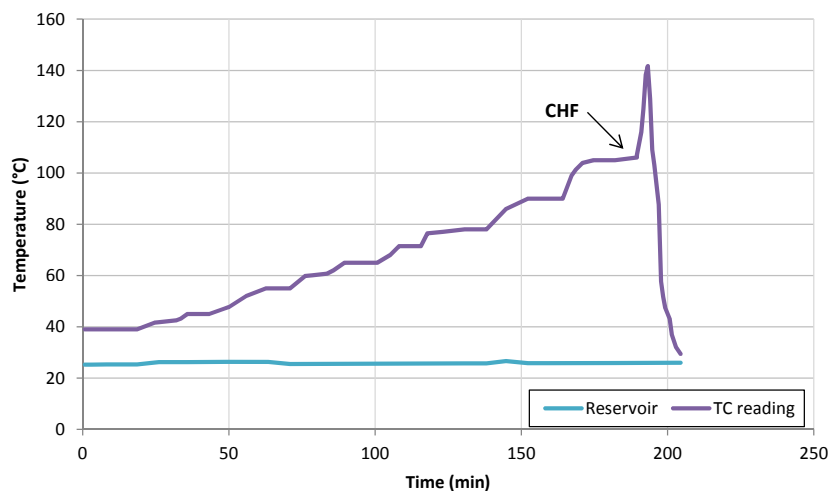
Figure 3.11: Example readings

3.3 Heat Loss and Measurement Error

Heat loss in the system is predicted by 3-D finite element modeling. Commercial software ANSYS is used to model spraying chamber and the heater with the flat surface configuration (Fig. 3.12).
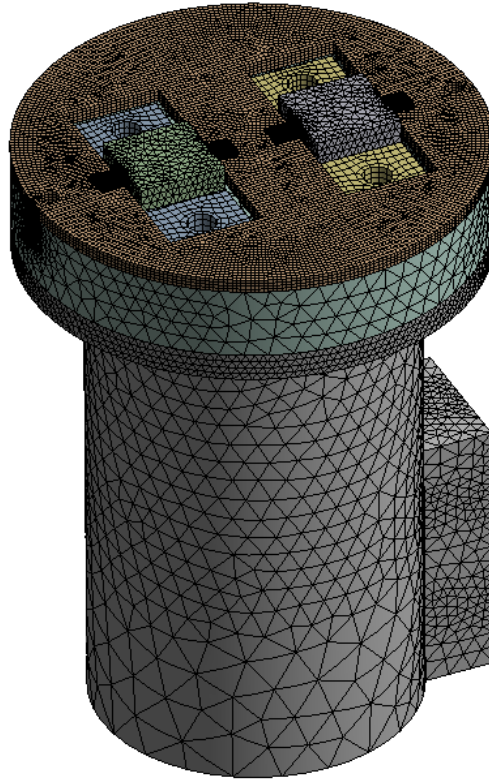
Figure 3.12: FEM Model of the Spraying Chamber

Four different materials are used in the analysis model. Heaters are modeled as two separate parts. Flange of the heaters are made of copper and top of the heater is made of beryllium oxide. Thermal conductivity values of copper, beryllium oxide, PCB and Teflon are 400, 248, 0.4 and 0.25 W/mK respectively. Since Teflon has a very low thermal conductivity, it can be considered as an insulator, hence it is assumed adiabatic. The free convection heat transfer coefficient of 10 $W/(m^2K)$ is defined for the other exposed surfaces. For sprayed surface overall heat transfer coefficient is found by iterative process. One set of the experiment is chosen in which heat flux is 68.9 W/cm^2 and surface temperature is 91 °C. Since heat input and temperature of the

surface is known, a number of analysis are done and overall heat transfer coefficient is assumed about 10500 $W/(m^2 K)$. Result of FEM analysis is shown in the Figure 3.12.
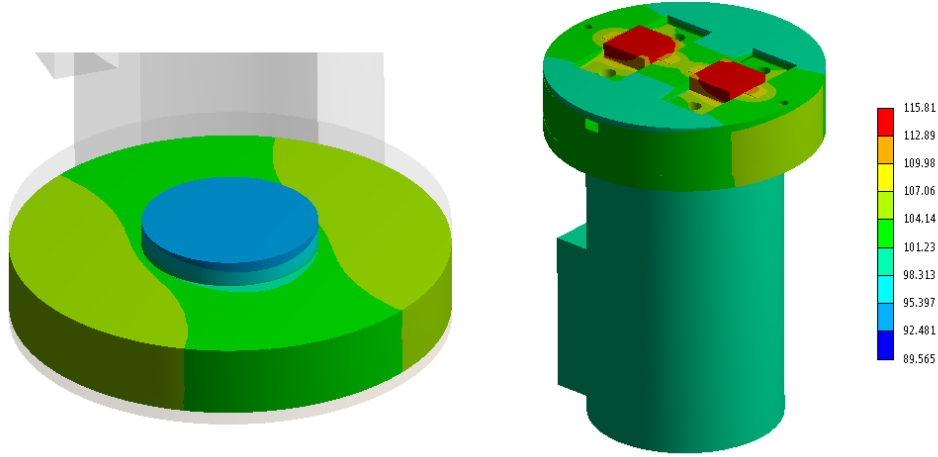
Figure 3.13: FEM results of flat surface (left) and whole model (right)

These results show that heat flux obtained in the system is 71.2 W/cm^2. Corresponding error is 3.2% in terms of maximum heat flux. Hence, heat loss to the surroundings can be assumed very low.

Pressure transducer used in the experiment has an accuracy of 0.1% FSO (Full scale output) (±0.0025 bar). J type thermocouples used in the surface temperature measurements has an accuracy of ±1°C.

SIEMENS SITRANS F C corriolis mass flow meter is calibrated for spray fluid at the beginning of the experiments. Its read errors are ≤ 0,1% kg/s of flow rate and ≤ 0.0015% g/cm^3 of density error according to datasheet.

CHAPTER 4

DISCUSSION OF RESULTS

4.1 Experimental Results

In the experiments dielectric fluid is the fluorocarbon perfluorohexane which is known as FC-72 manufactured by 3M [60]. Physical properties of FC-72 and water are given for comparison in the Table 4.1. Experiments are conducted at room temperature which is kept stable about $25°C$.

Table 4.1: Physical Properties of FC-72 [60]

Fluid Properties	FC-72	Water
Boiling Point @ 1 atm ($°C$)	56	100
Density x10^{-3} (kg/m^3)	1.68	0.997
Specific Heat x10^{-3} (J/kgK)	1.088	4.179
Thermal Conductivity ($W/m - K$)	0.0545	0.613
Dynamic Viscosity x10^4 (kg/ms)	4.5	8.55
Heat of Vaporization x10^{-4} (J/kg)	8.79	243.8
Surface Tension (N/m)	0.01	0.075
Dielectric Constant	1.72	78

The test flow rates chosen are 0.25, 0.35, and 0.40 lpm (liters per minute). Corresponding pressure values are 1.5, 2 and 2.5 bar. These pressure values are capable of creating a high-quality spray to form a full solid cone which was depicted in Figure

41

3.6. In Figure 4.1, the flow rate and pressure values are matched to nozzle performance graphics which is given by the manufacturer [61].
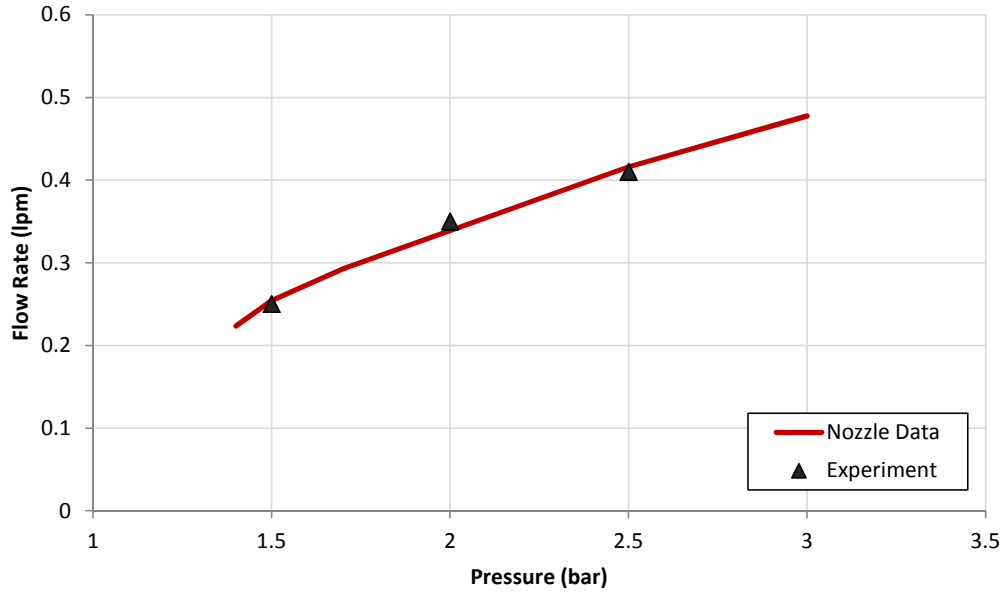
Figure 4.1: Nozzle pressure drop verification

Heat input to the surfaces is changed by increasing the voltage across the resistor. Since given load and structure (area of the heaters) are constant at each voltage value, heat flux is also constant. Hence, in this study heat flux is calculated using frontal area which is the same for all surfaces, 3.14 cm^2. In other words, a heat flux is not calculated using heat transfer area (wetted surface area) for each surface arrangement since the heater area is constant. In Table 4.2, surface number and wetted surface area of each surface are given according to their geometries which are listed in Table 3.1.

Table 4.2: Experiment Geometries

Surface No.	Surface Geometry	Wetted Surface Area (cm^2)
#0	Flat	3.14
#1	Straight 1	6.29
#2	Straight 2	9.43
#3	Straight 3	15.72
#4	Cubic 1	6.26
#5	Cubic 2	9.38
#6	Holes 1	5.3
#7	Holes 2	7.74
#8	Radial 1	6.99
#9	Radial 2	10.83

To compare heat flux values with different surfaces, two enhancement factors are defined, *Heat Flux Enhancement* (HE) and *Area Enhancement* (AE) in Equations 4.1 and 4.2 respectively. Heat Flux Enhancement is defined as the proportional increase of heat flux relative to the heat flux value of flat surface. Similarly, Area Enhancement is defined as the ratio of wetted surface area of the each surface to the wetted surface area of flat surface.

$$HE = \frac{q'' - q''_{flat}}{q''_{flat}} \times 100 \qquad (4.1)$$

$$AE = \frac{A_{surf}}{A_{flat}} \qquad (4.2)$$

4.1.1 Flat Surface Results

Firstly, heat flux and surface temperature values for flat surface (Surface #0) are given in the Figure 4.2. The figure clearly shows that as the flow rate increases from 0.25 lpm to 0.40 lpm, heat flux also increases as expected. Heat flux values for different

flow rates are tabulated in the Table 4.3. The maximum heat flux measured is 92.3 W/cm^2. In addition, surface temperature difference between flow rates at a certain heat flux has an increasing trend after $60°C$ that is the end of subcooling regime. However, maximum surface temperatures for all cases are close to each other.

Table 4.3: Surface #0 Heat Flux Values

Flow Rate (lpm)	**Heat Flux** (W/cm^2)
0.25	69.8
0.35	82.9
0.40	92.3
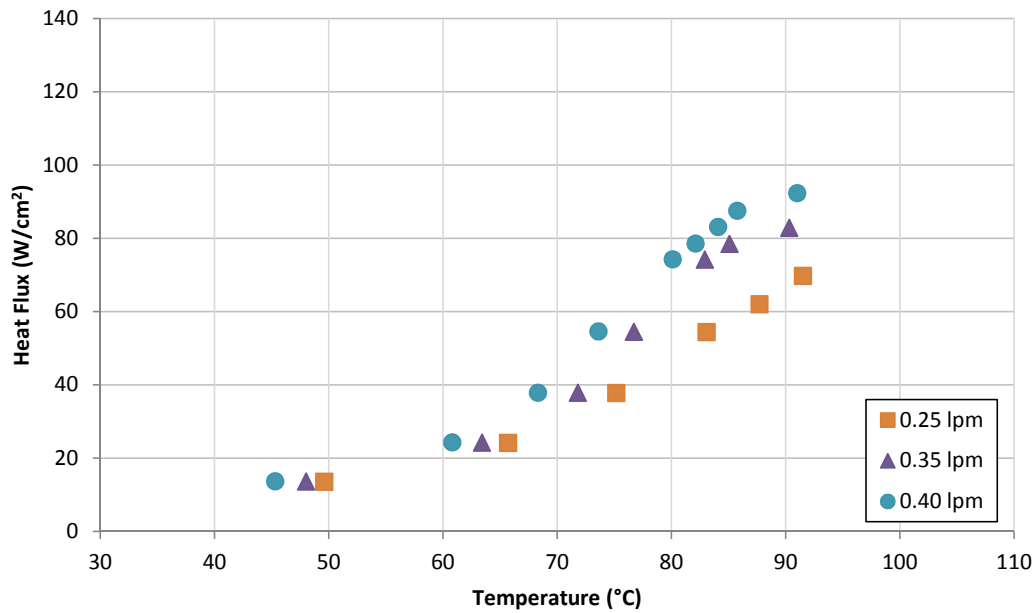
Figure 4.2: Heat Flux as a function of Surface Temperature for Surface #0

Although there are few empirical heat flux prediction for spray cooling applications in the literature due to its complicated nature, Estes and Mudawar [34] have a good prediction "'Volumetric Flux Model (VFM)"' of heat flux with an $\pm 30\%$ error. Estes and Mudawar used FC-72 as a working fluid and the same nozzle with this experiment. Later, Visara and Mudawar [48] have modified the subcooling term in VFM (2009) from 0.0019 to 0.0050. The new correlation is given in the Equation 2.13.

Flat surface results for three flow rates are compared with the two VFM models in the Figure 4.3. Error lines are plotted for the VFM (1995). Derivation of VFM is given in the Appendix A.
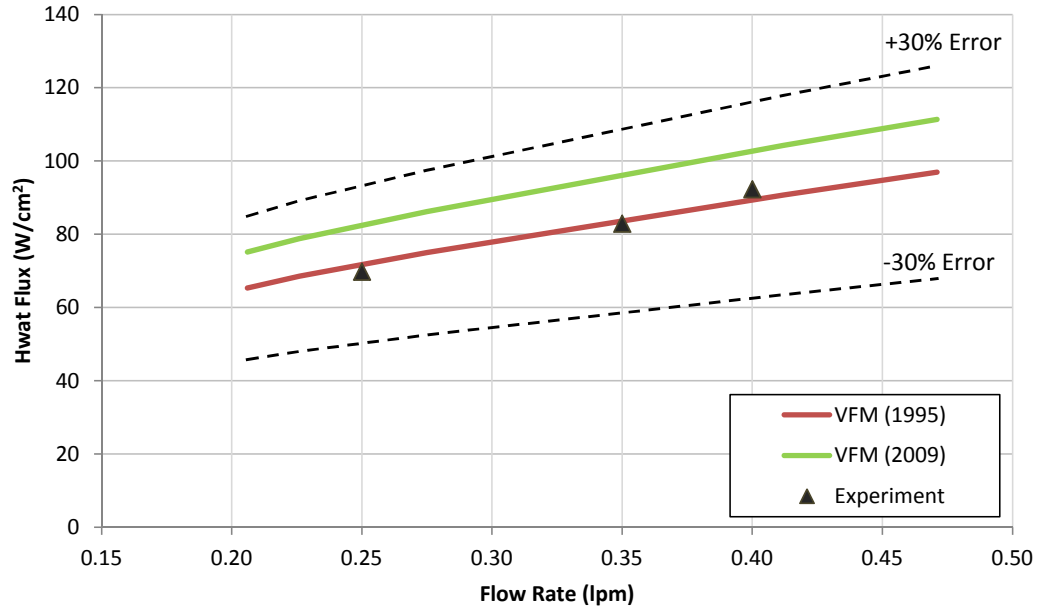
Figure 4.3: VFM Model comparison for Surface #0

Two VFM models show good agreement with the experimental data. The earlier correlation (Eqn. 2.10) fits perfectly with flat surface results. However, as a result of increased subcooling effect which is single phase convection prior to nucleation, heat flux values shifted up for the modified correlation (Eqn. 2.13). Two VFM model have similar trend and experimental data of flat surface are in the limit of error. Since, there is no experimental verification of Visaria's work [48], it is better to rely on earlier VFM model of Estes [34]. In VFM (1995) model heat fluxes are 73.7 W/cm^2, 85.8 W/cm^2 and 91.9 W/cm^2 with errors of 5.2%, 3.4% and -0.4% respectively. This verification may help to have a reliable comparison of finned surfaces with the flat surface results.

4.1.2 Straight Fin Results

Results of all straight finned surfaces, Surface #1, #2 and #3, are given in Figures 4.4, 4.5 and 4.6. Maximum heat fluxes, area enhancement (AE) and heat flux enhance-

ment (HE) values are summarized in the Table 4.4.

Table 4.4: Maximum Heat Flux at 0.40 lpm

Surface	Heat Flux (W/cm^2)	AE	HE (%)
#1	95.5	2.00	3.47
#2	106.3	3.00	15.17
#3	130	5.00	40.85

In the Figure 4.4, the increase in the wetted area of Surface #1 shows slight increase in heat flux values. This surface have a similar trend for different flow rates compared with Surface #0. However, it should be noted that surface temperatures at low heat fluxes are decreased compared to Surface #0. The maximum heat flux obtained in Surface #1 is 95.5 W/cm^2. In Surface #1, AE is about 2 times of Surface #0 whereas HE is just 3.47% of flat surface.
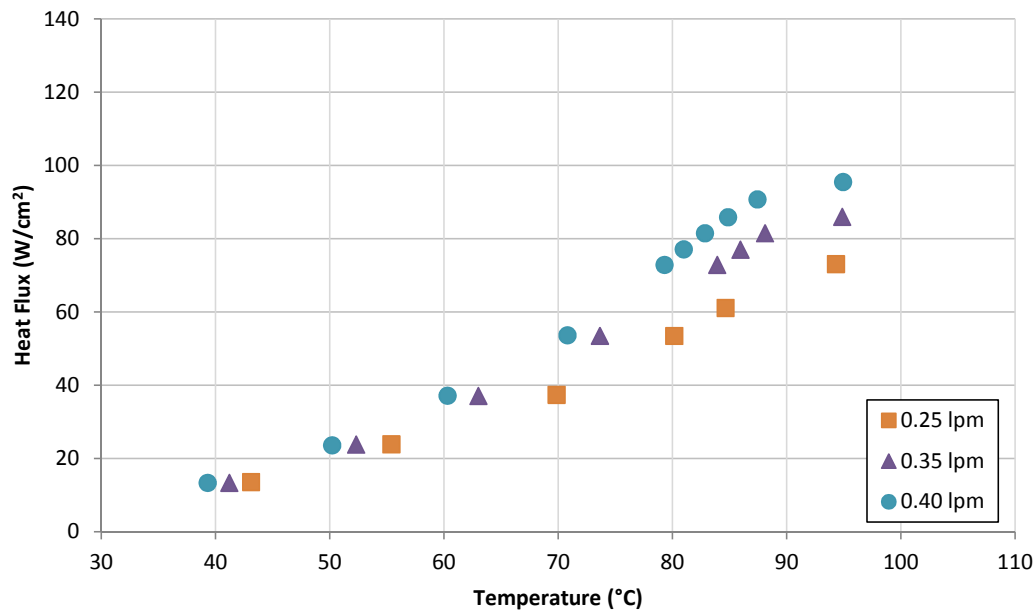
Figure 4.4: Heat Flux as a function of Surface Temperature for Surface #1

Surface #2 has the same characteristic with Surface #1 as it can be seen from the Figure 4.5. The maximum heat flux is increased to 106.3 W/cm^2. Compared to Surface #1 heat flux enhancement is increased to 15.17% when the area enhancement is 3.00.

46
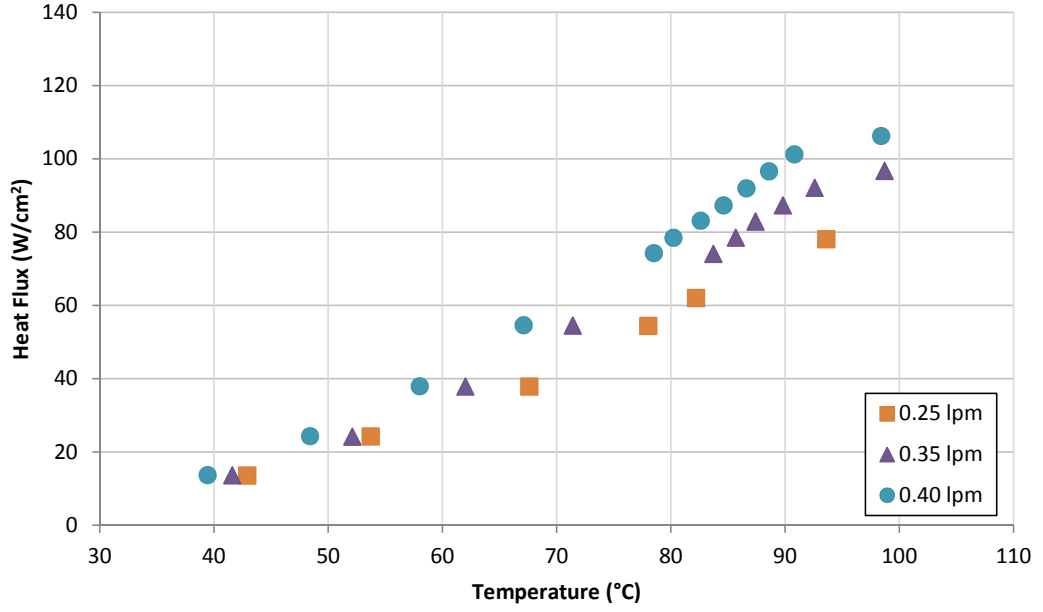
Figure 4.5: Heat Flux as a function of Surface Temperature for Surface #2
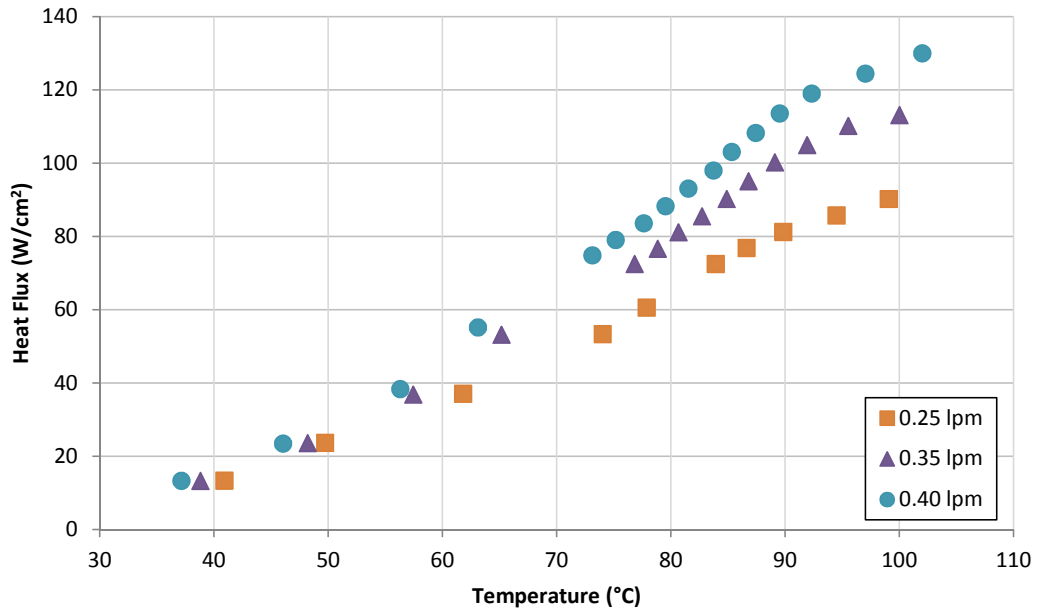
Figure 4.6: Heat Flux as a function of Surface Temperature for Surface #3

In the Figure 4.6, heat flux increase is much more obvious with the increasing flow rate compared to other straight finned geometries, which results in maximum heat flux value, 130 W/cm^2, among surfaces #1 to #3. Since the AE is the highest for the straight finned geometries, the highest HE value is obtained which is 40.85%.

47

Straight fin results show that there is certain increase in heat flux values relative to flat surface. However, the most important outcome of these results is that the area enhancement is not directly related to heat flux enhancement.

4.1.3   Cubic Fin Results

Heat flux values for different flow rates of two cubic finned surfaces, Surface #4 and #5, are given in the Figures 4.7 and 4.8, respectively. Maximum heat fluxes, area enhancement (AE) and heat flux enhancement (HE) values are summarized in the Table 4.5.

Table 4.5: Maximum Heat Flux at 0.40 lpm

Surface	Heat Flux (W/cm^2)	AE	HE (%)
#4	98.2	1.99	6.36
#5	103.4	2.99	11.98

Surface #4 results are presented in the Figure 4.7. It has the same trend with Surface #0 with slight increase in heat flux values. Maximum heat flux obtained is 98.2 W/cm^2 at a flow rate of 0.4 lpm. While area enhancement factor is nearly the same as Surface #1, HE is doubled -increased to 6.36%- compared to Surface #1.

Again Surface #5 has the same characteristics with Surface #4 as it can be seen from the Figure 4.8. Maximum heat flux is increased to 103.4 W/cm^2 with this surface arrangement. Heat flux enhancement is increased to 11.98% when area enhancement is 2.99.

Comparing straight and cubic finned surfaces while wetted surface area values are almost the same, heat flux enhancement values show different trend. In both Surface #1 and #4, although AE is almost 2 for both surfaces, HE is increased from 3.47% to 6.36%. However, with the same area enhancement of 3, HE is decreased from 15.17% to 11.98%. This unusual trend in this results may be attributed to the flow distribution on straight on cubic structures.

Figure 4.7: Heat Flux as a function of Surface Temperature for Surface #4
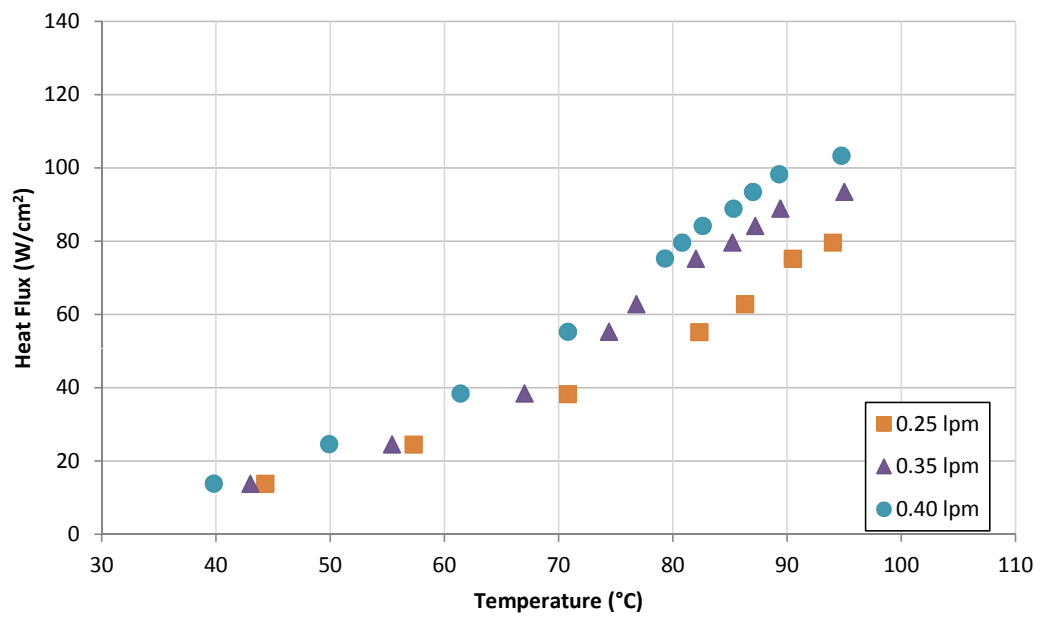
Figure 4.8: Heat Flux as a function of Surface Temperature for Surface #5

4.1.4   Holes Results

Results of surfaces with holes, Surface #6 and #7, are given in the Figures 4.9 and 4.10. Maximum heat fluxes, area enhancement (AE) and heat flux enhancement (HE)

49

values are summarized in the Table 4.6.

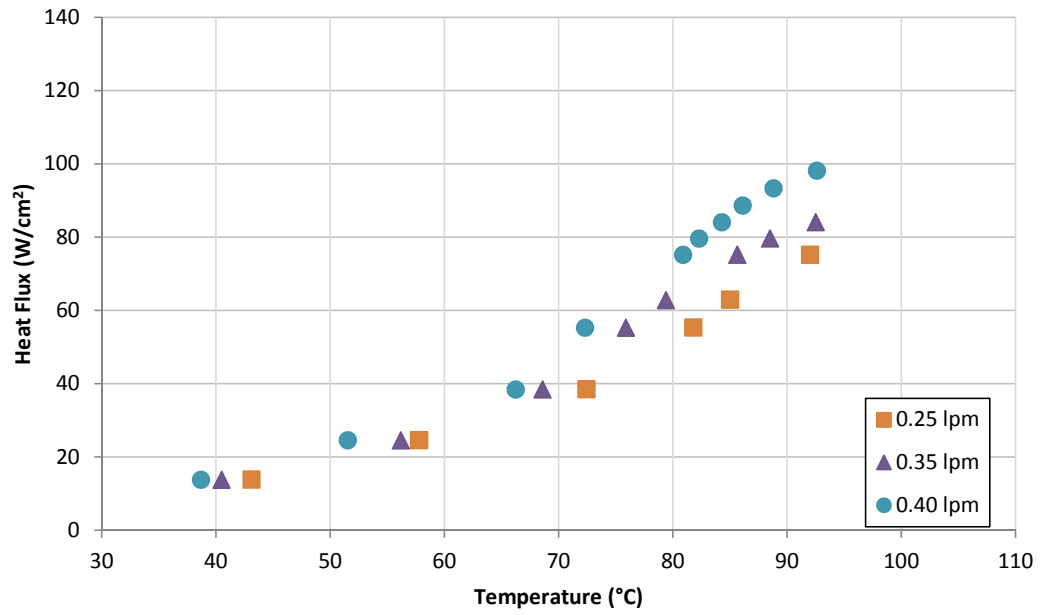**Table 4.6:** Maximum Heat Flux at 0.40 lpm

Surface	Heat Flux (W/cm^2)	AE	HE $(\%)$
#6	93.7	1.69	1.55
#7	98.3	2.46	6.49

Heat flux value in Surface #6 is increased to 93.7 W/cm^2 with an area enhancement of 1.69. As a result of low area enhancement value, lower heat flux enhancement is expected which is only 1.55%. However, as it can be seen from Figure 4.9, flow rate values do not alter heat flux values much when compared to other surface arrangements.
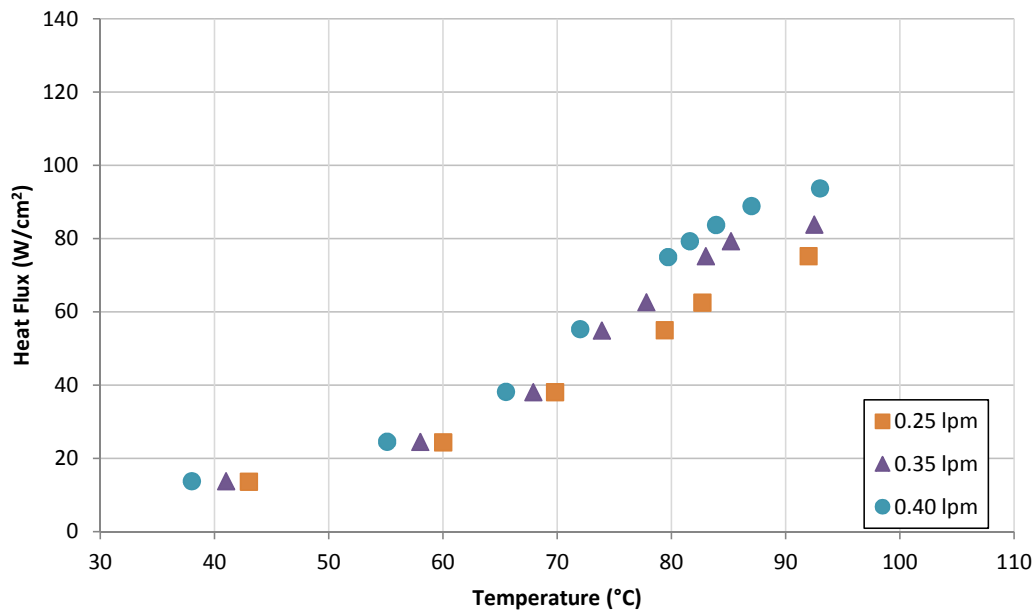
Figure 4.9: Heat Flux as a function of Surface Temperature for Surface #6

Similarly, heat flux values increase are very limited for different flow rates in the Figure 4.10. Maximum heat flux in Surface #7 is 98.3 W/cm^2 which corresponds to 6.49% heat flux enhancement. Again there is no linear dependence between AE and HE values when compared to other surfaces. Apart from other surfaces studied, surfaces with holes have different structures in fact. The presence of holes on the surface is affecting boiling regime by creating voids. The reason of low HE values

may be due to a decrease in wetted surface area with the presence of voids.
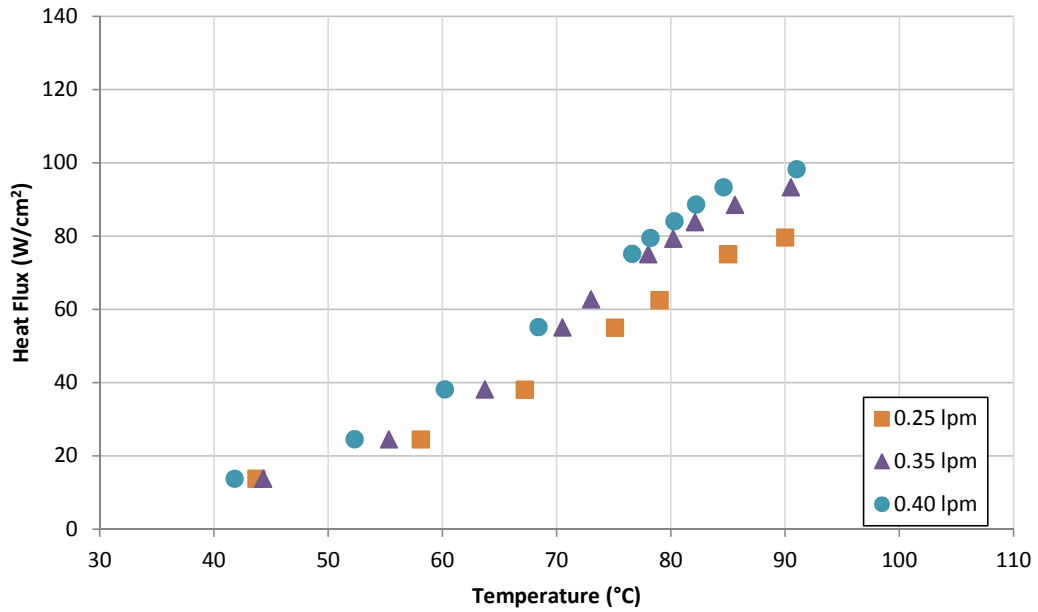
Figure 4.10: Heat Flux as a function of Surface Temperature for Surface #7

4.1.5 Radial Fin Results

The last sets of surfaces are radial fins. In the Figure 4.11 and 4.12 results of Surface #8 and Surface #9 are presented. Maximum heat fluxes, area enhancement (AE) and heat flux enhancement (HE) values are summarized in the Table 4.7.

Table 4.7: Maximum Heat Flux at 0.40 lpm

Surface	Heat Flux (W/cm^2)	AE	HE (%)
#6	108.9	2.22	18
#7	123.2	3.45	33.5

Surface #8 increased maximum heat flux to 108.9 W/cm^2 with an area enhancement of 2.22. This surface follows similar trend with straight fin surfaces as shown in the Figure 4.11. When compared to Surface #3 in terms of heat flux values, with less area enhancement in Surface #8, higher heat flux enhancement is obtained.

Again Surface #9 has the same characteristics as Surface #8 as it can observed from

51
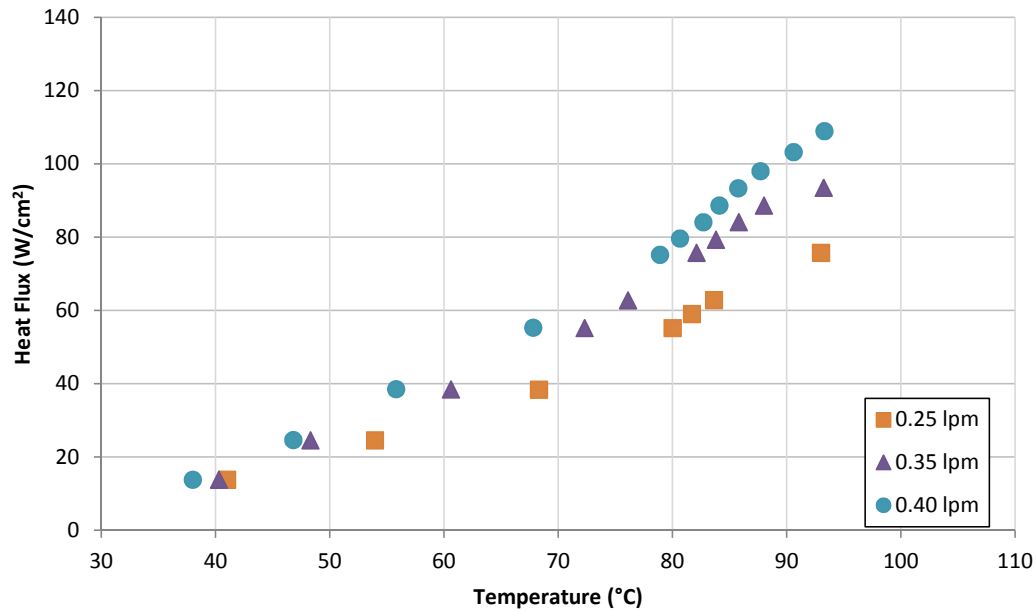
Figure 4.11: Heat Flux as a function of Surface Temperature for Surface #8

the Figure 4.12. The maximum heat flux is increased to is 123.2 W/cm^2 which corresponds to heat flux enhancement of 33.5%. at area enhancement of 3.45. With less AE compared to Surface #3 which was 5, the maximum heat flux increase is very close to Surface #9. Hence, these results show that it is possible to get much more heat flux enhancement with radial fins. The possible reason of enhancement increase in radial fins is that radial fins favor flow distribution which is in the direction of spray cone.
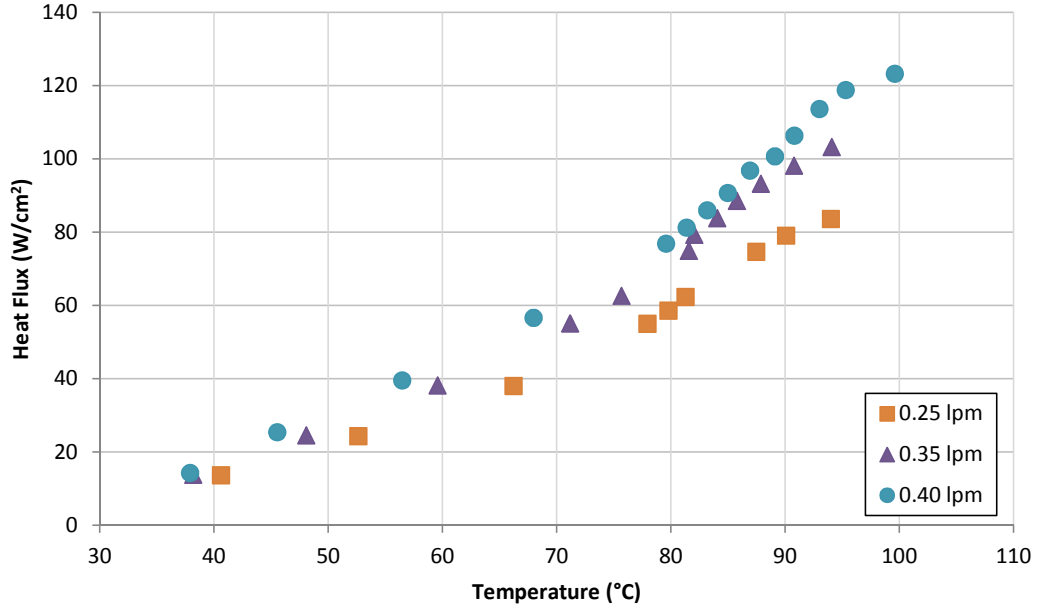
Figure 4.12: Heat Flux as a function of Surface Temperature for Surface #9

4.2   Summary and Discussion of the Results

To have better understanding, experimental results for all surfaces are listed in the Table 4.8. First observation about the experiments is that as the flow rate increases, heat transfer rate also increases. With increasing flow rate, higher quality spray is created at the nozzle. Finer fluid droplets increase heat transfer area that results in higher heat flux values for increased flow rate.

Since spray cooling is convective process with boiling, total wetted area increase in the surfaces certainly increases maximum heat flux. Different types of surfaces are compared in the Figures 4.13, 4.14 and 4.15 at different flow rates. Surface arrangements show similar trend with increasing flow rate. At subcooling regime (below 60°C) results for all surfaces are similar, there is no significant enhancement in heat flux values. Surface temperature are decreased because of increased heat transfer area as expected. However, in two-phase regime, surface effects become visible with the increasing flow rate. Surface #3 has the maximum wetted area with highest heat flux enhancement value of 40.85%. Results shows that surface temperature decreases with increasing wetted area and flow rate for all surface types. In practical applications, using finned surfaces will greatly increase cooling performance. Using such surfaces

Table 4.8: Results of all surfaces at 0.40 lpm flow rate

Surface	Type	Area (cm^2)	Heat Flux (W/cm^2)	HE (%)	AE
#3	Straight	15.72	130.0	40.85	5.00
#9	Radial	10.83	123.3	33.53	3.45
#8	Radial	6.99	109.0	18.05	2.22
#2	Straight	9.43	106.3	15.17	3.00
#5	Cubic	9.38	103.4	11.98	2.99
#7	Holes	7.74	98.3	6.49	2.46
#4	Cubic	6.26	98.2	6.36	1.99
#1	Straight	6.29	95.5	3.47	2.00
#6	Holes	5.3	93.7	1.55	1.69
#0	Flat	3.14	92.3	-	-

will certainly reduce surface temperature of the components at the same load. Temperature decrease in the electronic components will increase reliability and efficiency of electronic devices. These results show that using straight fins is very simple and efficient way to increase heat flux or reducing temperature of the devices.

However, as previously discussed, heat flux and area enhancement do not have linear trend. There is no well explained mechanism of surface enhancement in the literature because of the complex nature of spraying cooling. Previous studies show that heat transfer is directly related to the liquid film on the surface [62]. Finned surfaces greatly effect liquid film form and flow characteristics on the surfaces. This phenomenon is clearly observed in these experiments which have the same area enhancement values (straight and cubic fins). Fluid flow and liquid residence on the heated surface can be related to difference in heat transfer and area enhancement values. Depending on fluid flow rate, additional surfaces can hold liquid on the surface much longer. This may result longer sensible heating of the sprayed fluid. In addition to liquid residence time on the surface, heat transfer in multiphase region may
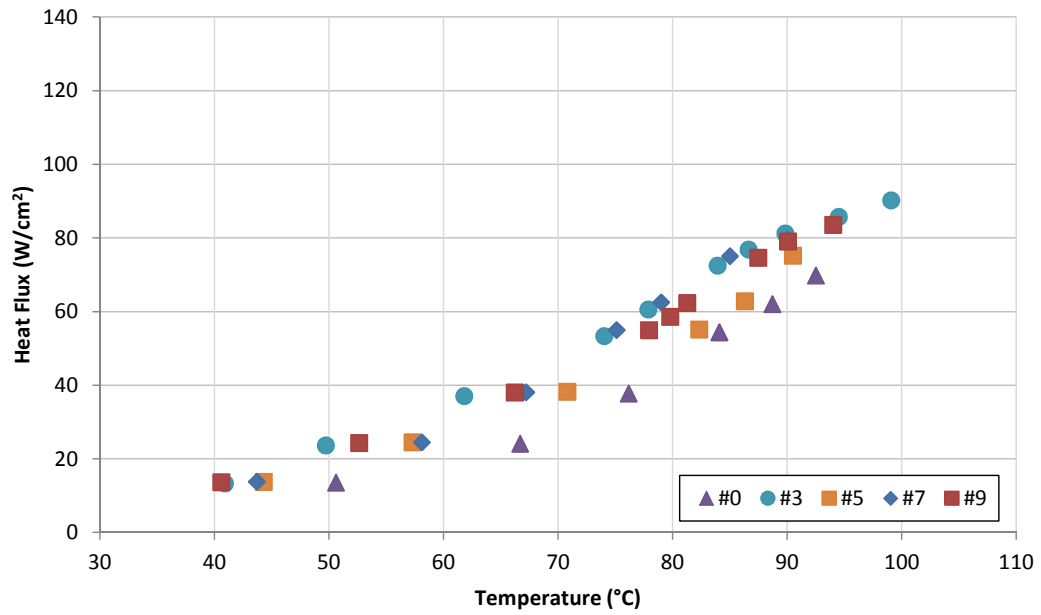
Figure 4.13: Comparison of heat flux values for different types of surfaces at 0.25 lpm
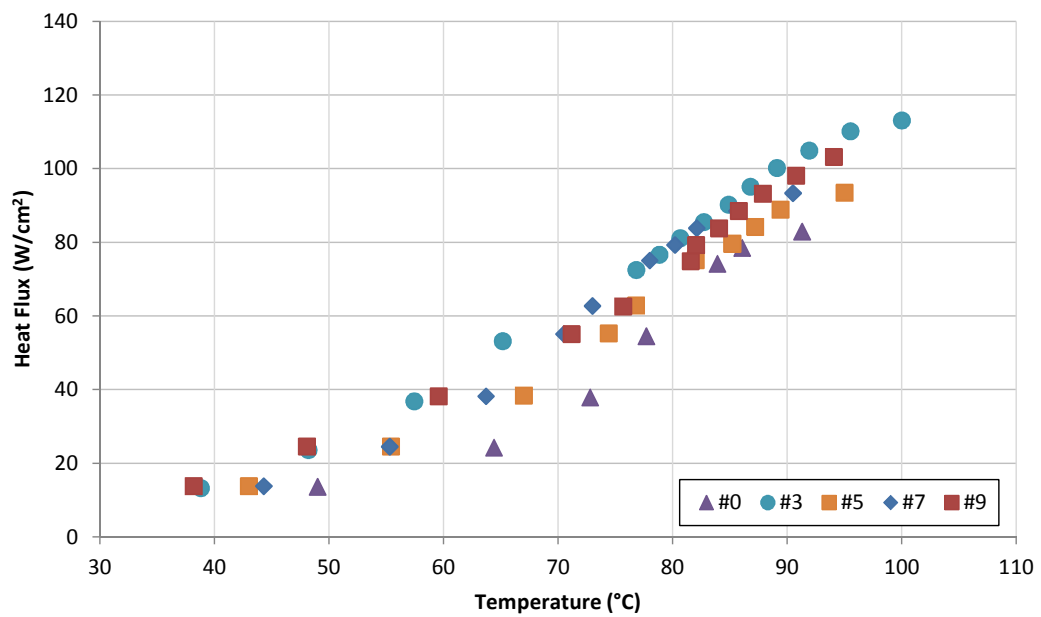
Figure 4.14: Comparison of heat flux values for different types of surfaces at 0.35 lpm

be increased by added nucleation sites on the surface. Yet there is no visualization in these experiments, it is hard to make interpretation of boiling process on extended
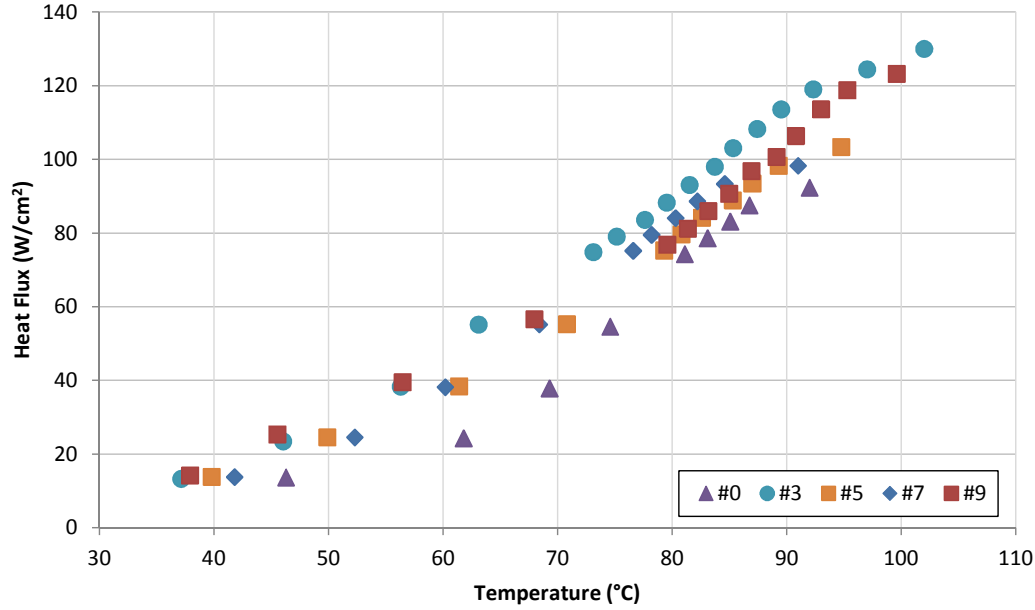
Figure 4.15: Comparison of heat flux values for different types of surfaces at 0.40 lpm

surfaces. However, difference in heat transfer and area enhancement values can not be explained by only this mechanism. As it can be seen from the Table 4.8, radial fins have higher HE values, although they have lower area enhancement values compared to straight or cubic fins. This might be related to fluid flow and drainage on the surface. Other than area increase, since spray cooling is convective process, convection coefficient is also changing for different surfaces. Convection coefficient is directly affected by fluid velocity. Channels formed on the surfaces decreases drainage area that increases fluid velocity in the channel. Radial fins work in the direction of the flow that velocity in the channel of the sprayed fluid is higher than other structures. This mechanism explains high HE value in radial fins although they have low area enhancement values.

Another important outcome of these experiments is the pressure change in the system. First prototype of experimental setup had a smaller reservoir and accumulator assembly unit. Since compactness of the systems is the main aim of this study, 0.1-liter reservoir with one bellow is used which is shown in the Figure B.1.

However, in earlier experiments with different flow rates, pressure change occurred

56

in the system. The main reason of this problem is the temperature increase in the reservoir. It should be noted that, in these experiments flow rates are low and FC-72 has very low specific heat value compared to water and other cooling liquids. For that reason, temperature increase at the exit of condenser is inevitable. Since the volume of reservoir is small, hot liquid coming from the condenser increases reservoir temperature quickly. In the Figure B.2 pressure and fluid temperature change are given for the flow rates of 0.35 and 0.45 lpm. According to these results, pressure increase in the system is about 15% with 6 °C temperature increase.

This pressure increase affects nozzle and boiling performance greatly which is unacceptable for experimental purposes. Possible reason of this problem is that hot liquid coming from condenser increases reservoir temperature and low heat of vaporization of FC-72 cause excess gas in the system. Bellow used in the reservoir can not compensate volume increase which results in an increase in pressure.

To overcome this problem, size of the reservoir and number of bellows are increased which is the current design of reservoir. Since the volume of reservoir is increased, temperature of the fluid do not change thus pressure is stable. During experiments, pressure and temperature of the reservoir are monitored and no significant changes were observed.

In practical applications 3-liter reservoir is very large for a compact cooling system. However, the pressure increase is inevitable in such a closed system. To eliminate temperature increase in the system huge condensers are needed which will be in contradiction with the compactness of the system. Since it is hard to keep temperature constant in a small reservoir, pressure increase will be present in real applications. High pressure in the reservoir can damage the system and may cause a leakage either gas or liquid. When designing a spray cooled system, pressure change must be taken into account for the performance of the cooling.

In addition to the temperature increase in reservoir, storage conditions of spraying cooling applications is also important. In electronics cooling, especially in military products, extreme temperatures occur up to 50°C typically while system is not working. Vapor pressure of the FC-72 which has a saturation temperature of 56°C will increase quickly. If pressure compensation is not enough in reservoir, fatal errors can

happen in such conditions. The risk of high pressure can be reduced by using different fluids, for example FC-84 whose saturation temperature is 80°C, yet surface temperature will be increased up to 150°C [63]. Nevertheless, most of the electronic components can not survive at a surface temperature of 150°C. FC-72 is the best spraying fluid for spray cooling at low surface temperature. In other words, pressure must be controlled carefully in closed loop spray cooling systems by relief valves or similar techniques. Hence much more complex system is inevitable for a compact spray cooling.

CHAPTER 5

CONCLUSION

5.1 Remarks

Emerging technology pushes electronics industry towards miniaturizing and increasing power requirement that result in high heat fluxes. Yet current cooling methods fall behind for certain applications. As discussed in this study, there are too much parameters and limitations to select appropriate cooling system for high heat flux application. At this point, spray cooling offers effective solution for electronics cooling. Despite its complex theory, spray cooling is advantageous with high cooling capacity.

During the study, a simple and application oriented test setup is constructed. Developed test setup performed very well in experiments. For enhancement of spray cooling ten different surface structures are tested. Depending on surface type a noticeable increase is observed. Maximum heat flux of 130 W/cm^2 which corresponds to 40.85% enhancement compared to flat surface, is achieved using straight fins in spray cooling. This study revealed following outcomes,

- Heat flux certainly increases with increasing flow rate for all surfaces. With increasing momentum, finer droplets are formed which results in heat transfer area increase in the droplets. However, this effect is limited with the capacity of the nozzle. Moreover, with increasing flow rate spray efficiency (Eqn. 2.6) decreases as discussed earlier. Study is verified by using empirical VFM model. Very good agreement is observed with the experimental results.

- Area increase has a great effect in enhancement of spray cooling. Studies with

different surface structures showed that total wetted area increase in the surfaces certainly enhances heat transfer performance. Area enhancement is an effective mechanism in both subcooling and multi-phase regime. In current applications, utilizing spray cooling with extended surfaces are certainly advantageous due to lowered junction temperatures.

- Fluid flow on the surface is the most important phenomenon in extended surfaces. Besides in area enhancement, draining fluid velocity has a great effect in heat transfer on the surface. Although maximum heat flux is obtained by straight fins, radial fins have the best heat flux enhancement and area enhancement ratio. The possible reason for this is related to the flow direction and fluid velocity on the surface. Increasing fluid velocity on the surface favors convection coefficient for spray cooling.

- This enhancement mechanism is the easiest and simplest way to approach theoretical maximum heat transfer rate in spray cooling. With same components, coolant fluid and pumping power, 40.85% increase in cooling capacity is achieved. This enhancement can be utilized for compactness for current applications by reducing the size of the heat exchanger or pumping power.

- When considering liquid cooling systems, constructed spray cooling setup is very simple. Being a two-phase system requires pressure regulation only. Meaning that this system can be utilized for current single phase liquid cooling systems by controlling system pressure carefully in closed loop spray cooling systems with relief valves or similar techniques. However, this adds complexity to the system.

5.2 Future Work

Present work and other studies about enhanced surfaces have been performed by using small copper surface. However, in practical applications copper is not preferred due to its weight. In today's electronics, aluminum is the optimum thermal material considering its thermal conductivity and density value. Yet, aluminum creates localized hotspots when compared to copper which will result in high temperature

gradient on the surface. Future studies with aluminum surfaces may lead to a better understanding of spray cooling efficiency on localized heat sources.

Another possible future work may be the characterization of spray cooling of varying working pressure. As discussed in the last section of Chapter 4, pressure increase may happen in spray cooling applications. Extreme operating conditions may change the pressure level in system. Saturation temperature and flow pressure changes should be taken into account when designing a spray cooling application. Hence it should be studied well enough to predict best or worst cooling conditions of spraying system.

REFERENCES

[1] Gordon E. Moore. Cramming more components onto integrated circuits. *Proceedings of the IEEE*, 86(2):1, 1998.

[2] Gordon N. Ellison. *Thermal Computations for Electronics*. CRC Press, 2011.

[3] Bejan Adrian. *Heat Transfer*. John Wiley & Sons Inc, 1993.

[4] J. Saylor, A. Bar-Cohen, T. Lee, T. Simon, W. Tong, and P. Wu. Fluid selection and property effects in single- and two-phase immersion cooling. *IEEE Transactions on Components, Packaging and Manufacturing Technology*, 11:557–565, 1988.

[5] Wits W. Williams. *Integrated Cooling Concepts for Printed Circuit Boards*. PhD thesis, University of Twente, 2008.

[6] Emrah Alpsan. Experimental investigation and numerical analysis of microchannel heat sinks for phased array radar cooling applications. Master's thesis, METU, 2008.

[7] Laird Technologies. *Thermoelectrics - Structure and Function*, 2010.

[8] Andreas Engelhardt and Peter Collington. Advanced thermal management technologies a brief overview.

[9] Element Six. *CVD Diamond Delivers A Cool Competitive Advantage*. Element Six, 2013.

[10] Robert E. Simons. Direct liquid immersion cooling for high power density microelectronics, May 1996.

[11] Clemens J.M., Lasance, and Simons R.E. Advances in high performance cooling for electronics. *Electronics Cooling*, 11:22–39, 2005.

[12] D. Saums, S. Gill, T. Louvar, A. Sathe, and D. Thompson. Vaporizable dielectric fluid cooling of igbt power semiconductors for vehicle powertrains. *Proceedings of Fifth IEEE Vehicle Power and Propulsion Conference (VPPC)*, 2009.

[13] Issam Mudawar. Assessment of high-heat-flux thermal management schemes. *IEEE Transactions on Components and Packaging Technologies*, 24:122–141, 2001.

[14] Inc. Cray Research. *The CRAY-2 Computer System*. Cray Research, Inc., 1985.

[15] Ahmet Muaz Ates. Experimental comparison of fluid and thermal characteristics of microchannel and metal foam heat sinks. Master's thesis, Middle East Technical University, 2011.

[16] D. Saums. Vaporizable dielectric fluid cooling of igbt power semiconductors for vehicle powertrains. In *5th IEEE Vehicle Power and Propulsion Conference*, September 7-11, 2009.

[17] Darin Sharar, Nicholas Jankowski, and Brian Morgan. Review of two-phase electronics cooling for army vehicle applications. Technical report, Army Research Laboratory, 2010.

[18] Pais M.R., Chow L.C., and Mahefkey E.T. Surface roughness and its effect on the heat transfer mechanism in spray cooling. *Journal of Heat Transfer*, 114:211–219, 1992.

[19] Overholt M.R., McCandless A., Kelly K.W., Becnel C.J., and Motakef S. Micro-jet arrays for cooling of electronic equipment. In *3rd International Conference on Microchannels and Minichannels*, 2005.

[20] Huseyin Bostanci, David Van Ee, and Louis C. Chow. Spray cooling of power electronics using high temperature coolant and enhanced surface. *IEEE Transactions on Components and Packaging Technologies*, 2009.

[21] Zhibin Yan, Rui Zhao, Fei Duan, Teck Neng Wong, Kok Chuan Toh, Kok Fah Choo, Poh Keong Chan, and Yong Sheng Chua. *Two Phase Flow, Phase Change and Numerical Modeling*, chapter Spray Cooling, pages 287–310. InTech, 2010.

[22] Glassman B.S. Spay cooling for land, sea, air and space based applications, a fluid management system for multiple nozzle spray cooing and a guide to high heat flux heater design. Master's thesis, University of Central Florida, 2005.

[23] Issam Mudawar. Assessment of high-heat flux thermal management schemes. *IEEE transactions on Components and Packaging Technologies*, 24 (2):122–141, 2001.

[24] Azar K. Advanced cooling concepts and their challenges, 2002.

[25] Anderson T. M. and Mudawar I. Microelectronic cooling by enhanced pool boiling of a dielectric fluorocarbon liquid. *Journal of Heat Transfer*, 111:752–759, 1989.

[26] Zuo Z.J., North M.T., and Wert K.L. High heat flux heat pipe mechanism for cooling of electronics. *IEEE transactions on Components and Packaging Technologies*, 24:220–225, 2001.

[27] Tuckerman D.B. and Pease R.F.W. High-performance heat sink for vlsi. *IEEE Electron Device Letters*, 2:126–129, 1981.

[28] Riffat S.B. and Ma X. Improving the coefficient of performance of thermo-electric cooling systems: a review. *International Journal of Energy Research*, 28:753–768, 2004.

[29] Rainey K.N., You S.M., and Lee S. Effect of pressure, subcooling, and dissolved gas on pool boiling heat transfer from microporous square pin-finned surfaces in fc-72. *International Journal of Heat Transfer*, 46:23–25, 2003a.

[30] Sturgis J.C. and Mudawar I. Critical heat flux in a long, rectangular channel subjected to onesided heating - ii. analysis of critical heat flux data. *International Journal of Heat Mass and Transfer*, 42:1849–1862, 1999.

[31] Faulkner D., Khotan M., and Shekarriz R. Practical design of a 1000 w/cm2 cooling system. In *19th IEEE SEMI-THERM Symposium*, pages 223–230, 2003.

[32] Huimin Liu. *Science and Engineering of Droplets*. Noyes Publications / William Andrew Publishing, 1999.

[33] Chandrakant D. Patel and Cullen E. Bash. Spray cooling system for a device, 2002.

[34] K.A. Estes and I. Mudawar. Correlation of sauter mean diameter and critical heat flux for spray cooling of small surfaces. *International Journal of Heat and Mass Transfer*, 38(16):2985–2996, 1995.

[35] Ghodbane M. and Holman J.P. Experimental study of spray cooling with freon-113. *International Journal of Heat and Mass Transfer*, 34 (4/5):1163–1174, 1991.

[36] Chen R.H., Chow L.C., and Navedo J.E. Effects of spray characteristics on critical heat flux in subcooled water spray cooling. *International Journal of Heat andMass Transfer*, pages 4033–4043, 2002.

[37] Huimin Liu. *Science and Engineering of Droplets*. Noyes Publications / William Andrew Publishing, 1999.

[38] Johnathan Stuart Coursey. *ENHANCEMENT OF SPRAY COOLING HEAT TRANSFER USING EXTENDED SURFACES AND NANOFLUIDS*. PhD thesis, University of Maryland, 2007.

[39] Yang J., Chow L.C., and Pais M.R. Nucleate boiling heat transfer in spray cooling. *Journal of Heat Transfer*, 118:668–671, 1996.

[40] Rini D.P., Chen R.H., and Chow L.C. Bubble behavior and nucleate boiling heat transfer in saturated fc-72 spray cooling. *Journal of Heat Transfer*, 124:63–72, 2002.

[41] J. Sengupta, B.G. Thomas, and M. A. Wells. The use of water cooling during the continuous casting of steel and aluminum alloys. *Metallurgical and Materials Transactions A: Physical Metallurgy and Materials Science*, 36A:187–204, 2005.

[42] Jungho Kim. Spray cooling heat transfer: The state of the art. *International Journal of Heat and Fluid Flow*, 28:753–767, 2007.

[43] Holman J.P. and Kendall C.M. Extended studies of spray cooling with freon-113. *International Journal of Heat and Mass Transfer*, 36:2239–2241, 1993.

[44] Issam Mudawar and Rybicki J.R. Single-phase and two-phase cooling characteristics of upward-facing and downward-facing sprays. *International Journal of Heat and Mass Transfer*, 49:5–16, 2006.

[45] Mudawar I. and Valentine W.S. Determination of the local quench curve for spray-cooled metallic surfaces. *Journal of Heat Treating*, 7:107–121, 1989.

[46] Shedd T.A. and Pautsch A.G. Spray impingement cooling with single- and multiple-nozzle arrays. part ii: Visualization and empirical models. *International Journal of Heat and Mass Transfer*, 48:3176–3184, 2005.

[47] Issam Mudawar. Recent advances in high-flux, two-phase thermal management. *Journal of Thermal Science and Engineering Applications*, 5, 2013.

[48] Milan Visaria and Issam Mudawar. Application of two-phase spray cooling for thermal management of electronic devices. *IEEE Transactions on Components and PackagingTechnologies*, 34:784–793, 2009.

[49] Kurihara H.M. and Myers J.E. The effects of superheat and surface roughness on boiling coefficients. *AIChE Journal*, 6(1):83–91, 1960.

[50] Nakayama W., Daikoku T., Kuwahara H., and Nakajima T. Dynamic model of enhanced boiling heat transfer on porous surfaces. *Journal of Heat Transfer*, 102:445–450, 1980.

[51] Sodtke C. and Stephan P. Spray cooling heat transfer on micro structured surfaces. In *Proc. of 6th World Conference on Experimental Heat Transfer, Fluid Mechanics, and Thermodynamics*, Matsushima, Miyagi, Japan., April 17-21, 2005.

[52] Huseyin Bostanci, Daniel P. Rini, John P. Kizito, Virendra Singh, Sudipta Seal, and Louis C. Chow. High heat flux spray cooling with ammonia: Investigation of enhanced surfaces for chf. *International Journal of Heat and Mass Transfer*, 55:3849–3856, 2012.

[53] B.H. Yang, H. Wang, X. Zhu, Q. Liao, Y.D. Ding, and R. Chen. Heat transfer enhancement of spray cooling with ammonia by microcavity surfaces. *Applied Thermal Engineering*, 20:245–250, 2013.

[54] Augusto G. Ulson de Souza and Jader R. Barbosa Jr. Spray cooling of plain and copper-foam enhanced surfaces. *Experimental Thermal and Fluid Science*, 39:198–206, 2012.

[55] Eric Silk, Kenneth Kiger, and Jungho Kim. Overview of enhanced surface spray cooling with embedded and extended surface structures. *ASME International Mechanical Engineering Congress*, IMECE2004 Conference Proceedings, 2004.

[56] J.L. Xie, Y.B. Tan, F. Duan, K. Ranjith, T.N. Wong, K.C. Toh, K.F. Choo, and P.K. Cha. Study of heat transfer enhancement for structured surfaces in spray cooling. *Applied Thermal Engineering*, doi: 10.1016/j.applthermaleng.2013.05.047.

[57] Lin L., Ponnappan R., Yerkes K., and Hager B. Large area spray cooling. In *Proceedings of ASME IMECE, Anaheim, Ca*, IMECE2004-61753, 2004.

[58] Murat Cetin. Design and experimental investigation of a microchannel heat exchanger. Master's thesis, Midde East Technical University, 2010.

[59] Huseyin Bostanci, David Van Ee, Benjamin Saarloos, and Daniel Rini. Spray cooling of power electronics using high temperature coolant and enhanced surface. *IEEE*, 2009.

[60] 3M. *Electronic Liquid FC-72 Product Info*.

[61] Sprayings Systems. *Full Cone Spray Nozzles*.

[62] Chien L.H. and Webb R.L. A parametric study of nucleate boiling on structured surfaces, part i: Effect of tunnel dimensions. *Journal of Heat Transfer*, 120:1042–1048, 1998.

[63] Cagri Balikci. Experimental study of spray cooling of electronics over high heat fluxed surface. Master's thesis, Middle East Technical University, 2013.

68

APPENDIX A

DERIVATION OF VFM

The all derivations in Appendix A are carried out by Mudawar [47]

As a first step nomenclature for inclined spray is given in A.1.
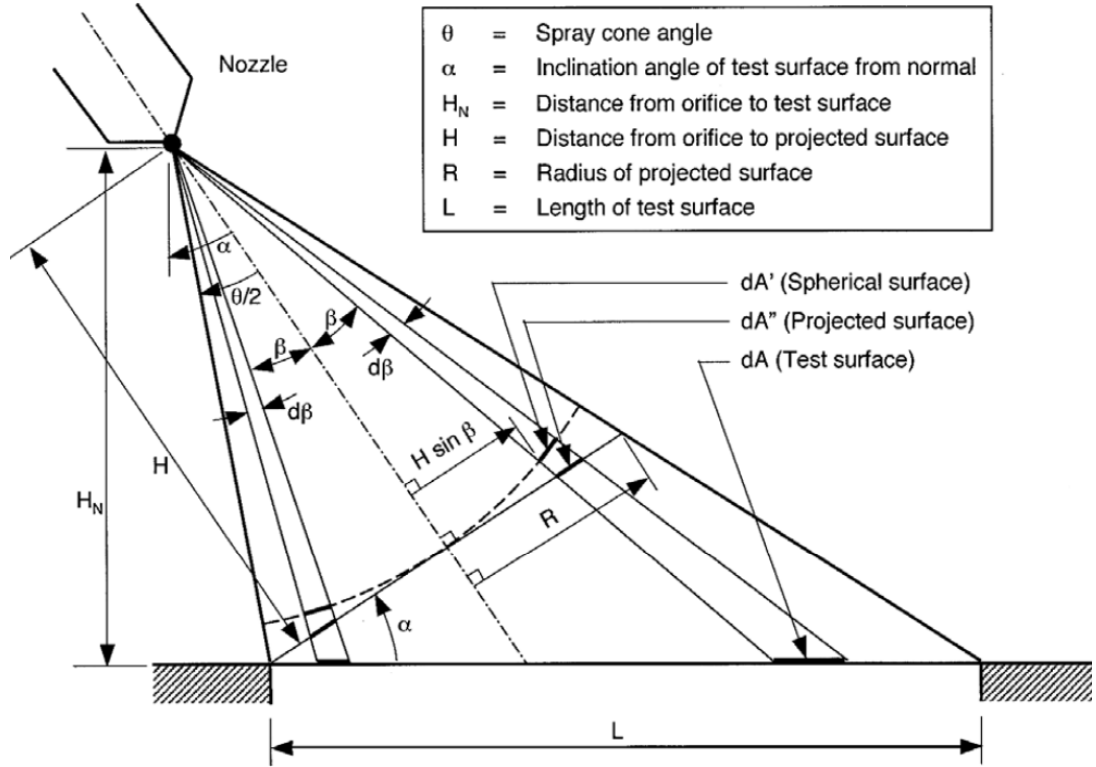
Figure A.1: Nomenclature for inclined spray

The projection distance H is found by following equation:

$$H = \frac{L}{2} \left[\cos \alpha \cot(\theta/2) - \sin \alpha \right] \qquad \text{(A.1)}$$

Then SMD is found.

$$\frac{d_{32}}{d_0} = 3.67 \left[We_{d_0}^{1/2} Re_{d_0} \right]^{-0.259} \tag{A.2}$$

Where;
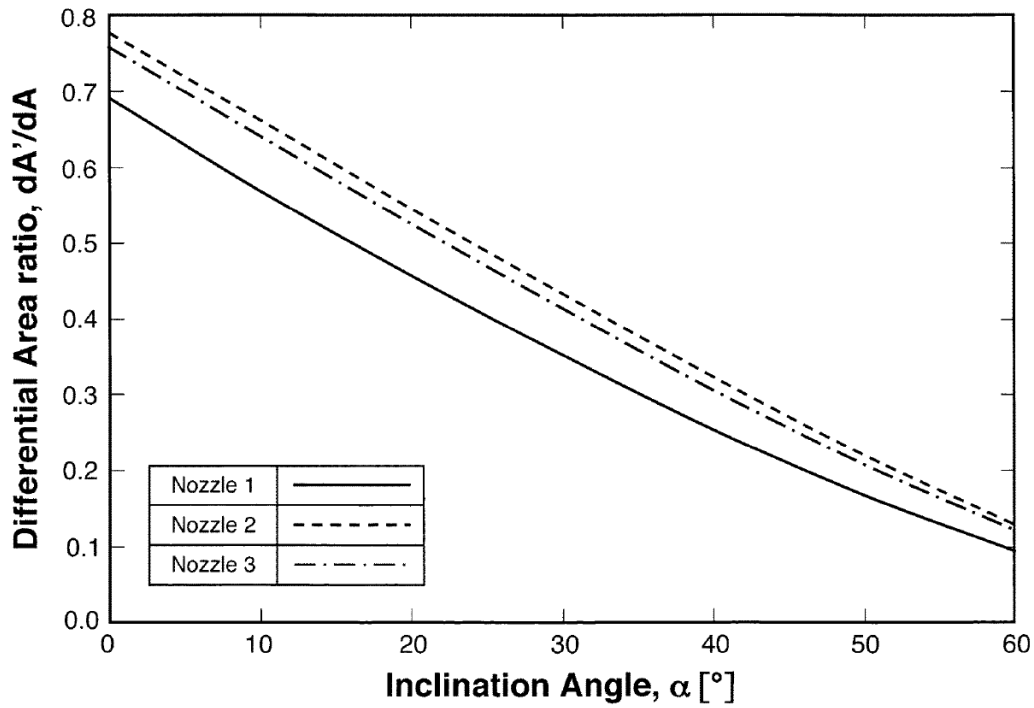
$$Re_{d_0} = \frac{\rho_f (2\Delta P/\rho_f)^{1/2} d_0}{\mu_f} \tag{A.3}$$

$$We_{d_0} = \frac{\rho_a (2\Delta P/\rho_f) d_0}{\sigma_f} \tag{A.4}$$

To find average volumetric flux:

$$\overline{Q}'' = \frac{Q}{\frac{\pi}{4} L^2 \cos\alpha \sqrt{1 - \tan^2\alpha \tan^2(\theta/2)}} \tag{A.5}$$

Then to find the other geometric factors, differential area ratio graph is offered. In Figure A.2 Nozzle 1 is the same nozzle used in current study.

Figure A.2: Differential area ratio with respect to inclination angle, dA'/dA

Then the geometric factors are found:

$$f_1 = \frac{1}{8}\left(\frac{L}{H}\right)^2 \frac{\cos\alpha\sqrt{1-\tan^2\alpha\tan^2(\theta/2)}}{1-\cos(\theta/2)}\frac{dA'}{dA} \tag{A.6}$$

$$f_2 = \frac{1}{\left[\frac{\pi}{4}\cos\alpha\sqrt{1-\tan^2\alpha\tan^2(\theta/2)}\right]} \tag{A.7}$$
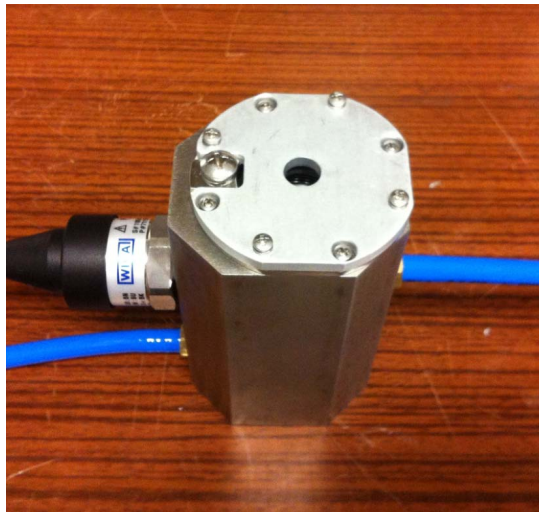
By using all equations above:

$$\frac{q_m''}{\rho_g h_{fg}\overline{Q}''} = 2.3\left(\frac{\rho_f}{\rho_g}\right)^{0.3}\left(\frac{\rho_f\overline{Q}''^2 d_{32}}{\sigma}\right)^{-0.35}\left(1+0.0019\frac{\rho_f C_{p,f}\Delta T_{sub}}{\rho_g h_{fg}}\right)\left(\frac{f_1^{0.30}}{f_2}\right) \tag{A.8}$$
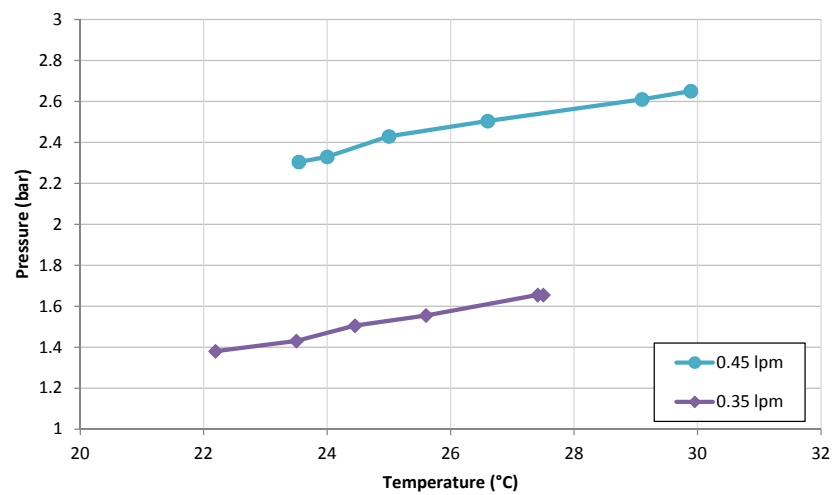
APPENDIX B

PRESSURE INCREASE

Figure B.1: First reservoir prototype

Figure B.2: Pressure and fluid temperature change in the system